



OPEN Biochemical and functional properties of vesicles from planktonic and biofilm phenotypes of *Limosilactobacillus reuteri* DSM 17938

Beatrice Marinacci^{1,9}, Chiara D'Ambrosio^{2,9}, Irene Vitale¹, Antonella Di Sotto³, Francesco Cairone⁴, Mattia Spano⁴, Simone Carradori¹, Andrea Scaloni², Marco Gulli³, Valentina Puca¹, Santolo Francati⁵, Monica Matuozzo², Ludwig Ermann Lundberg^{6,7}, Gianfranco Grompone⁷, Stefan Roos^{6,7} & Rossella Grande^{1,8}✉

Limosilactobacillus reuteri DSM 17938 is among the world's most studied probiotic strains and has been shown to provide several health benefits for the host. We have previously shown that the cell-free supernatant of *L. reuteri* DSM 17938 possesses antimicrobial activity and contains several bioactive compounds. Furthermore, the strain was shown to be a biofilm producer that releases both planktonic and biofilm Membrane Vesicles (MVs). In this study, membrane vesicles isolated from planktonic (pMVs) and biofilm (bMVs) phenotypes were comparatively investigated for their toxicity, ability to kill cancer as well as non-cancer cell lines and modulate phagocytosis in murine macrophages. Neither pMVs nor bMVs showed any in vivo toxicity in a *Galleria mellonella* model, and weakly affected cancer and noncancerous cell viability after both short- and long-term treatments. However, they were able to affect phagocytosis in lipopolysaccharide challenged RAW 264.7 macrophages, suggesting possible immunomodulatory properties. NMR-based metabolomic analysis of pMVs and bMVs identified and quantified engulfed compounds, mainly organic acids and amino acids, with lactate being the most abundant molecule in both vesicle types. bMVs contained higher concentrations of all measured metabolites compared to pMVs. Proteomic analysis of pMVs and bMVs described equivalent protein cargos, emphasizing quantitative compositional differences that presumably reflect the physiological state of each parent bacterial phenotype. Through the assignment of molecules possibly acting as mediators of immune/inflammatory responses in the host and/or modulating known beneficial effects of *L. reuteri*, important signaling functions of these vesicles were suggested. Finally, storage stability of MVs up to four weeks was established.

Keywords *Lactobacillus reuteri*, *Limosilactobacillus reuteri*, Extracellular membrane vesicles, Proteomics, Metabolomics, Cytotoxicity, Probiotics, Postbiotics, Immunomodulatory properties

Nowadays, the beneficial effects of probiotics on human health have been widely recognized. Probiotics can exert their function in different ways, for instance by modulating the immune system or affecting the microbiota by e.g. counteracting intestinal pathobionts and pathogens. In this context, different studies have proven pathogens inhibition and disease mitigating properties of probiotics^{1,2}. The health-promoting effects of probiotics are

¹Department of Pharmacy, "G. d'Annunzio" University of Chieti-Pescara, Chieti 66100, Italy. ²Proteomics, Metabolomics and Mass Spectrometry Laboratory, ISPAAM- National Research Council, Portici 80055, Italy. ³Department of Physiology and Pharmacology "V. Erspamer", Sapienza University of Rome, Rome 00185, Italy. ⁴Department of Chemistry and Technology of Drugs, Sapienza University of Rome, Rome 00185, Italy. ⁵Department of Agricultural and Food Sciences (DISTAL), University of Bologna, Bologna 40127, Italy. ⁶Department of Molecular Sciences, Uppsala Biocenter, Swedish University of Agricultural Sciences, Uppsala 750 07, Sweden. ⁷BioGaia AB, Stockholm SE-103 64, Sweden. ⁸Center for Advanced Studies and Technology, "G. d'Annunzio" University of Chieti-Pescara, Chieti 66100, Italy. ⁹Beatrice Marinacci and Chiara D'Ambrosio contributed equally. ✉email: rossella.grande@unich.it

strain-specific and can be mediated both through direct interactions with host cells and through the release of functional bacterial products^{2,3}. Among these, several metabolites and proteins (e.g. lactic acid, bacteriocins, quorum sensing molecules and enzymes) are known to have antioxidant, immunomodulatory and antibacterial properties and seem to exert antiproliferative activity on cancer cells^{3,4}. Membrane Vesicles (MVs) are also included in the Cell-Free Supernatant (CFS) of probiotics, thus their characterization is essential to better describe how bacteria interact with the host and the surrounding environment^{5,6}. All these active components can be part of postbiotic products that, according to the definition recently proposed by the International Scientific Association for Probiotics and Prebiotics, is “a preparation of inanimate microorganisms and/or their components that confers a health benefit on the host”⁷. Consequently, many scientists included the CFS of probiotic bacteria in postbiotic formulations whose composition varies according to the growth conditions and is unique for each bacterial strain^{8–10}.

More than 15 years of research recognizes the efficacy of *Limosilactobacillus reuteri* DSM 17938 in promoting beneficial effects on human health. For instance, Savino and coworkers have demonstrated that the administration of *L. reuteri* DSM 17938 alleviates symptoms in breastfed colicky infants, with a significant reduction of the daily crying time^{11,12}. A clinical trial also proved that a four-weeks supplementation of *L. reuteri* DSM 17938 promotes an increase of bowel movements in adults with chronic constipations, helping to increment the frequency of evacuations per weeks in treated patients¹³. Furthermore, *L. reuteri* DSM 17938 daily administration has been shown to reduce frequency and duration of diarrheal episodes in Mexican day school children aged 6–36 months. The trial has also evidenced that the supplementation of this probiotic strain could be related to the amelioration of other diseases, such as respiratory tract infections¹⁴.

As described above, probiotic properties can be promoted by released bacterial compounds. In this context, our previous works have already proved that the CFS of *L. reuteri* DSM 17938 exhibits both antimicrobial and antibiofilm activity against Gram-positive and Gram-negative bacteria^{15,16}. We showed that the CFS of *L. reuteri* DSM 17938 is directly involved in counteracting clinically relevant pathogens, and this activity can be related to the synergy between various CFS compounds. In our effort to further characterize the secretome of this bacterium, we have focused on *L. reuteri* DSM 17938 membrane vesicles. These lipid bilayer particles are released by bacteria and are loaded with macromolecules such as proteins, glycolipids, lipopolysaccharide (LPS) and nucleic acids; they can differ in dimension, biogenesis and composition depending on the producing strain¹⁷. MVs have been proposed as a system of communication between bacteria and with the host, involved in quorum sensing, biofilm formation and in the modulation of different biological processes⁶. As mentioned, MVs are also involved in microorganism-host interactions, and several authors have recently suggested that MVs released by probiotics may be of importance for the probiotic action^{18–20}. Accordingly, probiotic or postbiotic products containing MVs could potentially be used to reduce the risk for or ameliorate a wide range of diseases, such as chronic inflammatory conditions, neurological disorders, infections and cancer¹⁹.

Depending on its physiological state and the environmental conditions, *L. reuteri* DSM 17938 can have a planktonic or biofilm phenotype, both of which also produce MVs. In this work we have characterized and highlighted differences between planktonic membrane vesicles (pMVs) and biofilm membrane vesicles (bMVs). After isolation of the MVs, they were first comparatively assayed for in vivo toxicological properties in a *Galleria mellonella* model. Thereafter, the ability of pMVs and bMVs to inhibit various human gastro-intestinal cancer cell lines, including extrahepatic cholangiocarcinoma, pancreas adenocarcinoma, hepatoma and triple negative cancer, was evaluated. Tolerability of the MVs was also comparatively assessed in noncancerous cells. In addition, the ability of the MVs to modulate phagocytic properties of murine macrophages, both in the absence and presence of LPS from *Escherichia coli* O111:B4, was evaluated in terms of neutral red dye uptake²¹. Finally, the metabolomic and proteomic cargos of pMVs and bMVs were comparatively investigated to identify possible metabolites and proteins associated with the functional properties (Fig. 1).

Results and discussion

The workflow of the present study is shown in Fig. 1.

L. reuteri DSM 17938 MVs isolation and quantification

L. reuteri DSM 17938 pMVs and bMVs were isolated as previously described and further characterized for their physicochemical properties^{15,22}. The average size and concentration of nanoparticles were investigated via Nanoparticle Tracking Analysis (NTA), and pMVs had an average diameter of 85 ± 4 nm and a concentration of 1.83×10^{11} particles/mL, while the bMVs had an average diameter of 145 ± 2 nm and a concentration of 7.87×10^{10} particles/mL. A Transmission Electron Microscopy (TEM) analysis was performed in order to assess the morphology and the integrity of both MVs phenotypes (Fig. 2).

MVs from *L. reuteri* DSM 17938 are well tolerated by *G. mellonella* larvae

Freshly prepared *L. reuteri* DSM 17938 pMVs and bMVs were comparatively assayed for their in vivo toxicological properties in the *G. mellonella* in vivo model. All larvae were confirmed alive 4 days after treatment. As shown in Fig. 3A, no larvae died after receiving *L. reuteri*-derived MVs and the survival curves of the treated groups were comparable with that of the controls. At the same time, all larvae treated with DMSO died after the injection. These outcomes indicated no toxicity of MVs in *G. mellonella* at the concentration tested. In Fig. 3D–E–F–G, images of the larvae are shown at day 4 after treatment. The larvae appeared responsive to touch and were able to correct themselves when rolled onto their back; in addition, no color change was detected. Similar results were obtained in the *L. reuteri* DSM 17938 treated groups. As shown in Fig. 3B, no larvae died at 4 days post-infection. On the contrary, the infection performed with different concentrations of *Staphylococcus aureus* ATCC 43300 showed a decrease of larval survival over time, confirming previously published data (Fig. 3C)²³.

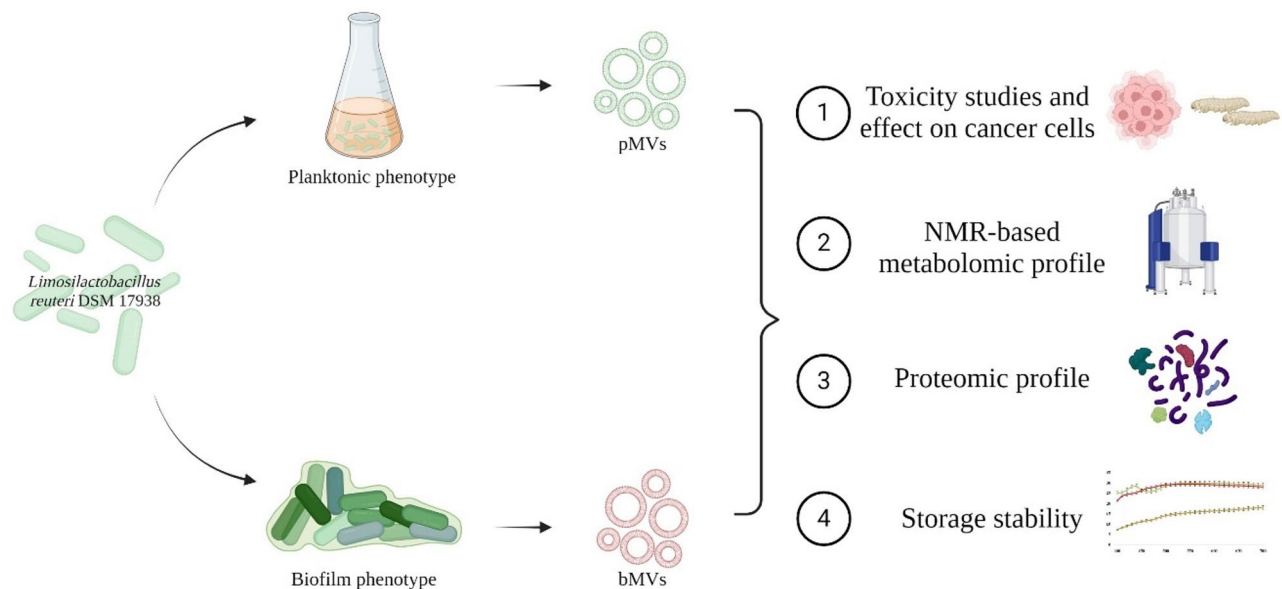


Fig. 1. Flowchart of this study. Membrane vesicles of the planktonic phenotype, pMVs; membrane vesicles of biofilm phenotype, bMVs.

These preliminary results highlight the safety of both pMVs and bMVs at a dosage corresponding to 10^8 MVs/larva which represents the highest dosage injectable.

Cytotoxicity studies

MVs effects on the viability of human cancer and noncancerous cells

The cytotoxicity of freshly prepared *L. reuteri* DSM 17938 pMVs and bMVs (concentration range of 1×10^5 to 1×10^9 MVs/mL in a 1X Dulbecco's Phosphate-Buffered Saline (PBS) solution) was investigated in different human cancer cell lines to highlight a possible antiproliferative activity; similar experiments were accomplished in noncancerous cells to test the tolerability of the treatment. The effect of the treatments was compared to PBS and doxorubicin ($10 \mu\text{g/mL}$), included as vehicle and positive controls, respectively. Doxorubicin is widely recognized as a standard cytotoxic agent with multifaceted mechanisms of action, including interference with DNA replication and repair, induction of oxidative stress, thus disrupting key processes involved in cell growth and proliferation²⁴.

According to the ISO 10,993–5:2009 for in vitro cytotoxicity studies, a higher than 30% inhibition of cell viability with respect to the vehicle control was considered as a biologically significant cytotoxicity (toxicity axis in Figs. 4, 5, 6 and 7)²⁵.

After 24 h exposure, both pMVs and bMVs were nontoxic up to the concentration of 1×10^7 MVs/mL in Bx-PC3 pancreas adenocarcinoma cells. In the same cells, bMVs produced a 10 to 20% inhibition of cancer cell viability starting from 1×10^8 MVs/mL, while pMVs showed early cytotoxicity signs only at the highest concentration of 1×10^9 MVs/mL (Fig. 4A). Similarly, both pMVs and bMVs were noncytotoxic to Mz-ChA-1 extrahepatic cholangiocarcinoma and HepG2 hepatoma cells up to the highest concentration (Fig. 4C and E); conversely about a 10% reduction of cell viability was produced in MDA-MB-468 triple negative cancer cells by the two highest concentrations of pMVs and only the highest concentration of bMVs (Fig. 4G). When the exposure was extended up to 72 h, no cytotoxicity signs were highlighted almost in all the tested cells, except for the highest concentration of pMVs and bMVs in Bx-PC3 cells and that of pMVs in MDA-MB-468 cells, which induced about 15% inhibition in cell viability (Figs. 4B, D, F and H).

In H69 cholangiocytes, both pMVs and bMVs showed weak cytotoxic effects after 24 h exposure, which were not observed after 72 h (Fig. 5). Indeed, the treatments usually resulted in less than 10% reduction in cell viability compared to the control, except for the two highest concentrations, where pMVs and bMVs induced 14% and 18% cytotoxicity, respectively (Fig. 5A). This evidence suggests that MVs were generally well-tolerated by noncancerous cells, with a slight lowering in cell viability that cannot be attributed to a biologically significant cytotoxic effect. The latter results confirmed the in vivo toxicity data for pMVs and bMVs evaluated in the *G. mellonella* model.

Emerging results highlight that probiotic bacteria may exhibit anti-cancer properties, owing to their ability to regulate inflammation, cell proliferation and apoptosis through the release of anti-cancer mediators^{19,26–37}. Among them, bacterial membrane vesicles have been found to be involved in both the pathogenesis and prevention of diseases such as cancers^{38,39}. Despite the cancer promoting abilities highlighted for MVs from *Bacteroides fragilis* (colorectal cancer), *Fusobacterium nucleatum* (colorectal and breast cancer) and *Helicobacter pylori* (gastric cancer), several probiotics have been found to be tumour-suppressive³⁹. Among them, Gurunathan and coworkers reported that *Bacillus licheniformis* nanovesicles induced a 50% inhibition in cell viability and

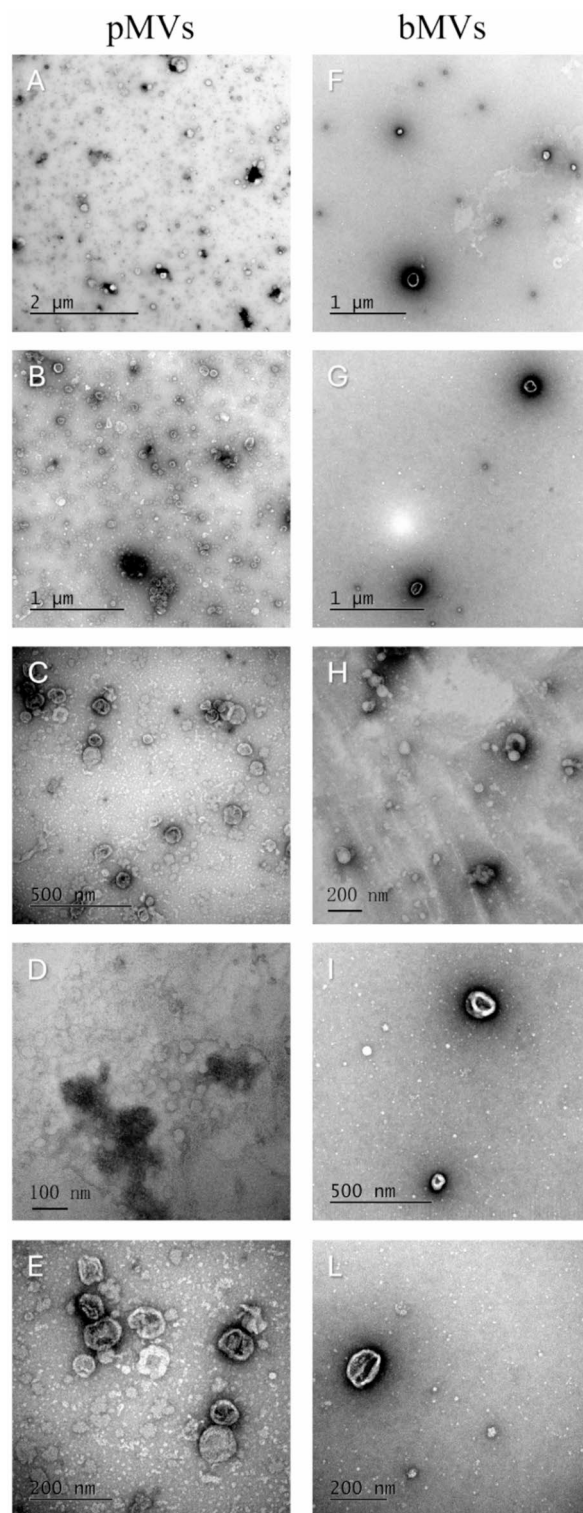


Fig. 2. Images of pMVs (A–E) and bMVs (F–L) obtained after negative staining and TEM analysis. (A) pMVs, scale bar 2 μm , magnification 13,000 \times . (B) pMVs, scale bar 1 μm , magnification 23,000 \times . (C) pMVs, scale bar 500 nm, magnification 49,000 \times . (D) pMVs, scale bar 100 nm, magnification 73,000 \times . (E) pMVs, scale bar 200 nm, magnification 98,000 \times . (F) bMVs, scale bar 1 μm , magnification 18,500 \times . (G) bMVs, scale bar 1 μm , magnification 23,000 \times . (H) bMVs, scale bar 200 nm, magnification 36,000 \times . (I) bMVs, scale bar 500 nm, magnification 49,000 \times . (L) bMVs, scale bar 200 nm, magnification 68,000 \times .

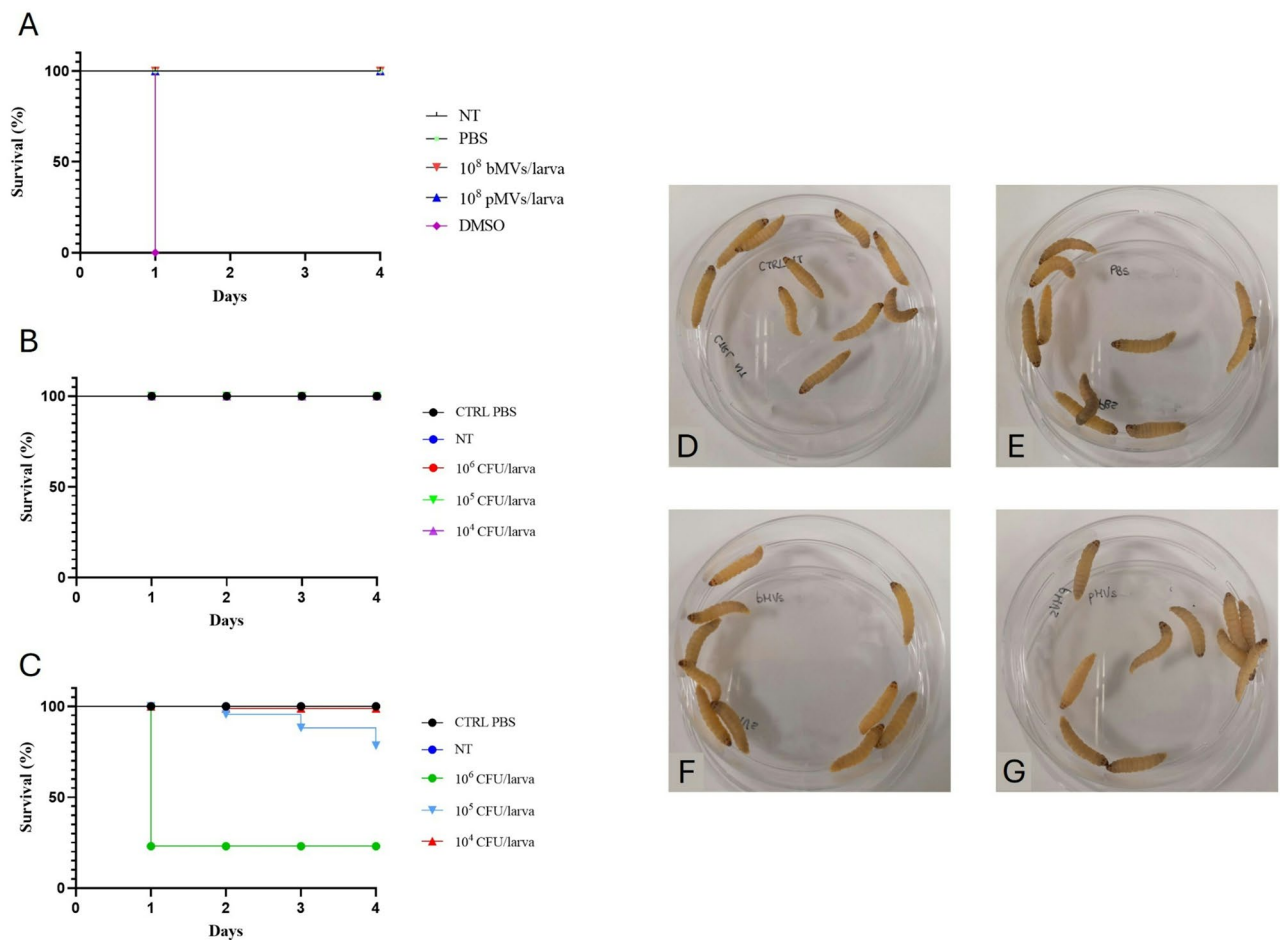


Fig. 3. (A) Effect of freshly prepared *L. reuteri* DSM 17938 MVs on *G. mellonella* survival (Kaplan-Meier survival curve) and *G. mellonella* larvae at day 4 after treatment with freshly prepared *L. reuteri* DSM 17938 MVs. (B) Effect of *L. reuteri* DSM 17938 on *G. mellonella* survival. (C) Effect of *S. aureus* ATCC 43300 on *G. mellonella* survival. (D) Non-treated larvae; (E) PBS-treated larvae; (F) bMVs-treated larvae; (G) pMVs-treated larvae.

proliferation in MDA-MB-231 and A549 cells⁴⁰. Keyani and colleagues highlighted up to a 60% reduction in cell viability of colorectal cancer cells by *Lactobacillus rhamnosus* GG MVs⁴¹, while Behzadi and coworkers reported about a 20% cytotoxicity and pro-apoptotic effects of MVs derived from *Lactocaseibacillus rhamnosus* GG in liver cancer HepG2 cells⁴². An and Ha showed that MVs from *Lactobacillus plantarum* (recently renamed as *Lactiplantibacillus plantarum*) induced a 20% inhibition of cell viability in the human HCT116 colon adenocarcinoma cell line with almost a 60% inhibition in the derived 5-fluorouracil resistant HCT116 cell line⁴³. The marked effect in resistant cells was ascribed to a reduction in the glucose metabolism, associated with a downregulation of pyruvate dehydrogenase kinase 2 expression, suggesting a possible interest in *L. plantarum* MVs to overcome chemoresistance⁴⁴. Accordingly, MVs from *L. plantarum* (Bio-67374) were able to block the proliferation and decrease the glycolytic metabolic reprogramming of human colon cancer cell lines by modulating the SIRT5/p53 axis⁴⁵. Moreover, MVs from *Lactocaseibacillus paracasei* PC-H1 exhibited about a 20% inhibition in cell viability of colorectal cancer cells and in xenograft mice; this effect was associated with a downregulation of the PDK1/AKT/Bcl-2 signaling pathway and a decrease in HIF-1 α -mediated glycolysis⁴³. Recently, the MVs from a *Lentilactobacillus buchneri* strain isolated from an Iranian yogurt were able to inhibit the cell viability of human gastric and colon cancer cell lines (AGS and HT-29, respectively), likely by inducing a cell cycle arrest in G0/G1 phase, apoptosis, and block of cell migration⁴⁶. Although it is known that MVs may deliver diverse bioactive agents, including bioactive proteins, nucleic acids, lipids and metabolites, the true compounds involved in the highlighted anticancer properties have not been clarified.

Under our experimental conditions, pMVs and bMVs from *L. reuteri* DSM 17938 caused up to a 20% decrease in the viability of pancreatic and mammary cancer cells. Specifically, bMVs were more efficacious against pancreatic cancer cells, whereas pMVs showed greater efficacy against mammary cancer cells. These results agree with previous evidence, highlighting anti-proliferative and pro-apoptotic effects of *L. reuteri* strains in diverse cancers^{27–29,36,37}; more recently, Yi et al. found that the extracellular vesicles from *L. reuteri* possessed

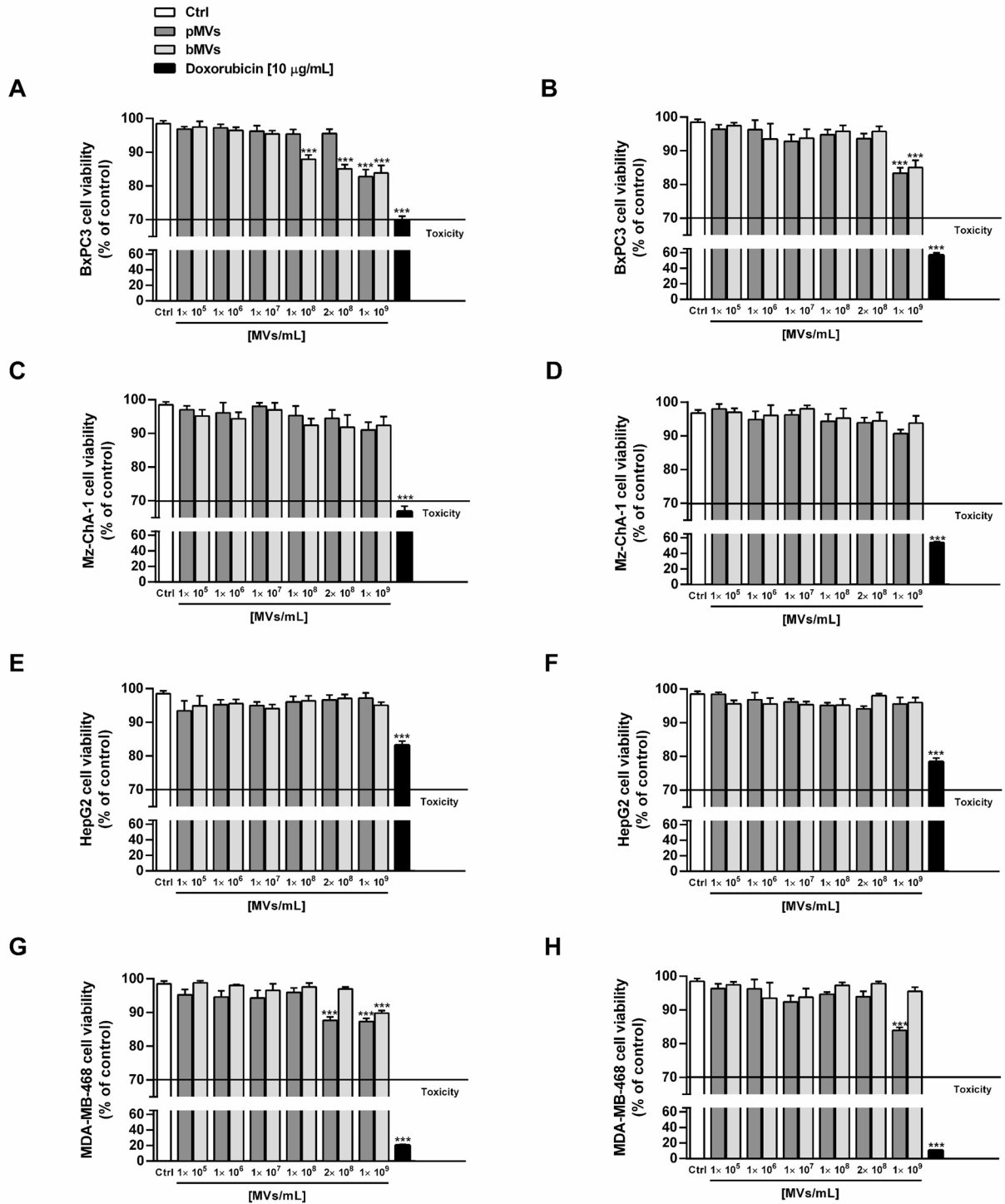


Fig. 4. Effect of freshly prepared *L. reuteri* DSM 17938 pMV and bMV and doxorubicin (black bar, 10 µg/mL) on human cancer cell viability after 24 h (A, C, E, G) and 72 h (B, D, F, H) exposure. In the negative control (Ctrl), the cells were treated with a 1X PBS solution. Bars represent the mean ± standard error of at least six measurements from two independent experiments. **A, B.** Bx-PC3 pancreas adenocarcinoma cancer cells. **C, D.** Mz-ChA-1 cholangiocarcinoma cells. **E, F.** HepG2 hepatoma cells. **G, H.** MDA-MB-468 triple negative cancer cells. *** $p < 0.001$ vs. Ctrl (ANOVA + Dunnett’s Multiple comparison post-test).

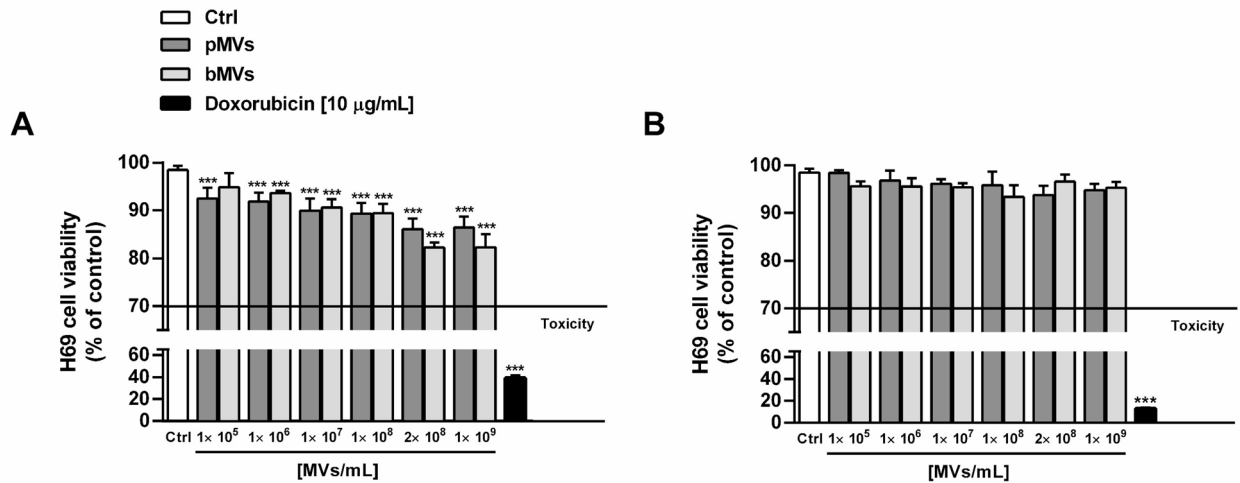


Fig. 5. Effect of freshly prepared *L. reuteri* DSM 17938 pMVs and bMVs and doxorubicin (black bar, 10 µg/mL) on the cell viability of noncancerous H69 cholangiocytes after 24 h (A) and 72 h (B) exposure. In the negative control (Ctrl), the cells were treated with a 1X PBS solution. Bars represent the mean ± standard error of at least six measurements from two independent experiments. *** $p < 0.001$ vs. Ctrl (ANOVA + Dunnett's Multiple comparison post-test).

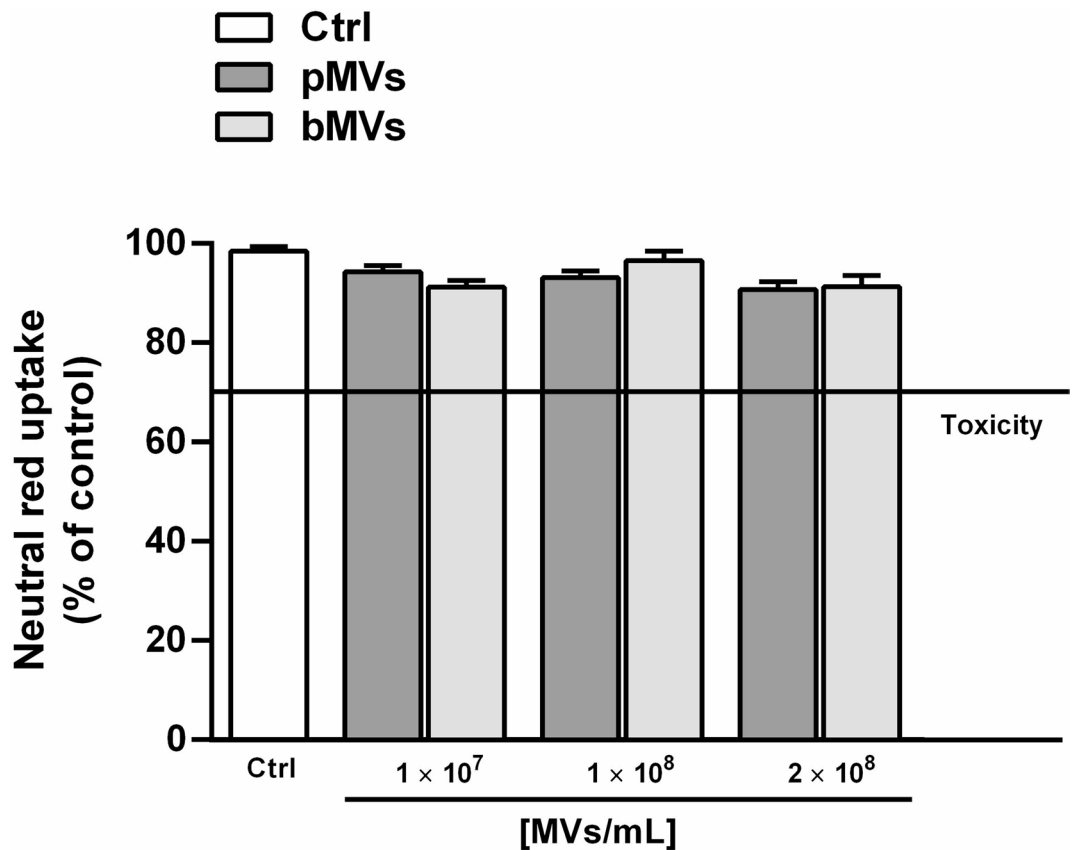


Fig. 6. Effect of freshly prepared *L. reuteri* DSM 17938 pMVs and bMVs on the neutral red dye uptake by murine RAW 264.7 macrophages. In the negative control (Ctrl), the cells were treated with a 1X PBS solution. Bars represent the mean ± standard error of at least six measurements from two independent experiments.

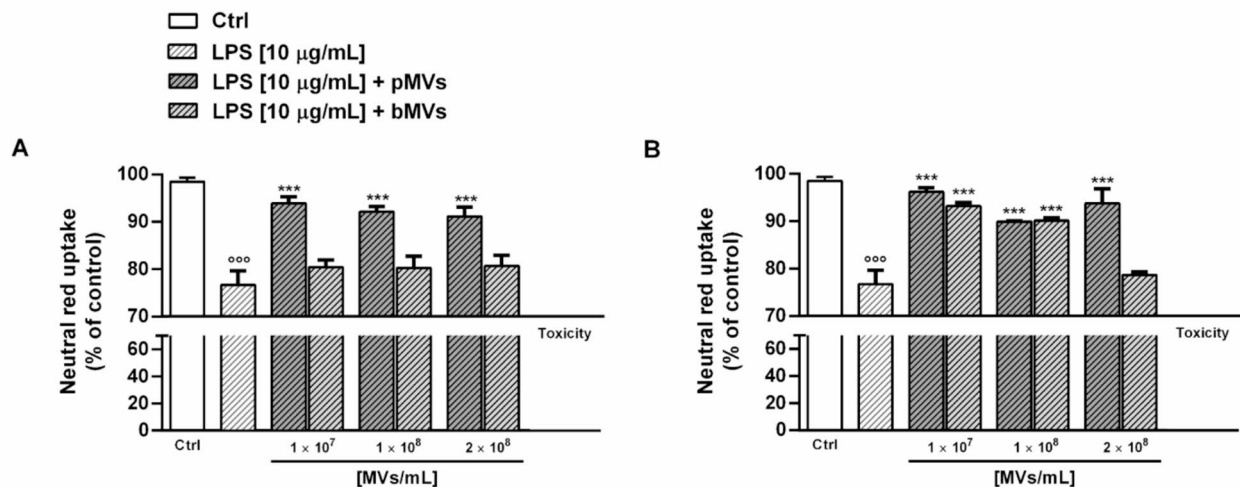


Fig. 7. Effect of pre- (A) and co-treatment (B) of freshly prepared *L. reuteri* DSM 17938 pMV and bMV on the neutral red dye uptake by LPS-induced murine RAW 264.7 macrophages. In the negative control (Ctrl), the cells were treated with a 1X PBS solution. Bars represent the mean \pm standard error of at least six measurements from two independent experiments. $^{\circ\circ\circ}p < 0.001$ vs. Ctrl (t-Student test); $^{***}p < 0.001$ vs. LPS (ANOVA + Dunnett's Multiple comparison post-test).

antiproliferative, antimigration and proapoptotic effects in A549 cells, as well as antitumor activity in a xenograft mouse model⁴⁷.

Interestingly, we found that both types of MVs were weakly cytotoxic in noncancerous cholangiocytes only after a 24 h exposure, without effects after 72 h treatment, likely as a consequence of a cell recovery. Accordingly, Kahouli and colleagues reported well tolerability of *L. reuteri* NCIMB 701,359 in CRL-1831 epithelial normal colon cells³⁷. Based on the available data, we cannot rule out the possibility that MVs selectively affect critical targets for cancer cell survival. Further studies are needed to investigate these specific mechanisms and to clarify this issue.

Our findings also suggest that pMV and bMV from *L. reuteri* DSM 17938 possess distinct chemical and physical features that may account for the observed, albeit subtle, differences in their toxicity toward cancer cells. Both types of MVs from *L. reuteri* DSM 17938 were found to be a source of diverse organic acids, especially lactate, citrate and succinate, and amino acids, such as alanine and glycine, with higher amounts in bMV than pMV. Among them, organic acids have attracted great attention as both oncometabolites and regulators of cell cycle and cancer cell metabolism and survival^{48–50}. In this respect, both in vitro and in vivo studies showed that citrate possessed promising antitumor properties, being able to disrupt cancer metabolism, enhance apoptosis, neutralize tumor microenvironment (TME) acidity, and reduce tumor growth⁴⁹. However, conflicting evidence has been reported for lactate and succinate, being both potentially able to either interfere with tumor cell metabolism and promote tumor growth. For instance, high intracellular lactate levels may induce lactylation and increased expression of genes involved in angiogenesis, immune evasion, and metastasis⁵¹; moreover, the compound may control the cell cycle and proliferation⁵². Similarly, the intracellular accumulation of succinate seems to promote cancer growth and progression, through the activation of genes involved in angiogenesis, glycolysis, and adaptation to hypoxia⁵³. On the other hand, succinic acid exhibited antiproliferative properties and proapoptotic effects in various cancer models, among which breast, renal and lung cancer⁵⁴. Based on these findings, these compounds may contribute to the cell viability modulation by MVs from *L. reuteri* DSM 17938 in pancreatic and breast cancer cells. Their higher amounts in bMV with respect to pMV could explain the higher potency in pancreatic cells. Differences in the cancer cytotoxicity potency of pMV and bMV may also arise from their different size, which could influence their uptake efficiency by host cells. The diameter of bMV from *L. reuteri* DSM 17938, approximately double that of pMV, is similar to that reported for MVs from *L. buchneri* and *L. paracasei* PC-H1, which inhibited the viability of gastric adenocarcinoma and colon cancer cell lines⁴³; however, the true role of vesicle size in their bioactivities is unknown. Altogether, the obtained results suggest a potential ability of pMV and bMV to control cell viability and proliferation, potentially inducing a cell cycle arrest or apoptotic cell death, as previously reported for MVs from other lactic acid bacteria^{41,43}, although the specific underlying mechanisms require further exploration.

MVs effects on the uptake by RAW 264.7 murine macrophages

The effect of freshly prepared *L. reuteri* DSM 17938 pMV and bMV on the uptake by RAW 264.7 murine macrophages was evaluated by the Neutral Red Uptake (NRU) assay, a well-established method for assessing cell viability, wherein viable cells incorporate the neutral red dye, and internalize it inside lysosomes; thus, cytotoxicity arises because of the hindered dye uptake induced by the treatments⁵⁵. In the case of macrophages,

this assay may provide preliminary insights into their uptake capabilities, which are crucial for their immune defense function.

Under the experimental conditions used, the 24 h exposure to both pMVs and bMVs did not affect NRU until the highest concentration tested (Fig. 6); conversely, the tested MVs restored the basal NRU after a 24 h stimulation by LPS from *Escherichia coli* O111:B4 (10 µg/mL). Indeed, despite a 20% reduction induced by LPS, NRU was more than 90% in the presence of pMVs under both pre- and co-treatments (Fig. 7A and B) and in the presence of bMVs under co-treatment (Fig. 7B).

Although more targeted studies are needed to confirm the effects of *L. reuteri* DSM 17938 pMVs and bMVs on the phagocytic activity of murine macrophages, our results suggest possible immunomodulatory properties of the vesicles, as also reported in other studies^{56,57}.

In this respect, Kim and coworkers showed that MVs from *L. plantarum* APSulloc 331261 induced the secretion of the anti-inflammatory and immunomodulatory cytokines in human skin organ cultures and stimulated the transition of HP1 monocytes to the anti-inflammatory and immunomodulatory M2b macrophages⁵⁸. In addition, *L. plantarum* Q7-derived extracellular vesicles have also been shown to regulate intestinal microbiota and ameliorate inflammation in a mouse model of ulcerative colitis⁵⁹. Moreover, a dedicated study demonstrated that *L. reuteri* BBC3-derived MVs maintained the intestinal immune homeostasis against LPS-induced inflammatory responses in broilers⁶⁰. Others have also demonstrated the ability of *L. reuteri* to regulate the immune system in humans and animals^{61,62}.

Hu and colleagues proposed that MVs released by *L. reuteri* BBC3 may inhibit pro-inflammatory mediators produced by activated inflammatory cells and activate innate immune cells to produce immunoregulatory cytokines, ultimately leading to the development of regulatory T cells with anti-inflammatory activities⁶⁰.

In accordance with these findings, we found that pMVs and bMVs from *L. reuteri* DSM 17938 counteracted the pro-inflammatory stimulation induced by LPS by restoring the basal NRU abilities. LPS is known to polarize macrophages into M1 phenotype, which triggers an inflammatory response and releases pro-inflammatory factors⁶³. Under our experimental conditions, pMVs restored macrophage NRU impaired by LPS both in the pre- and co-treatment protocols, while bMVs only under co-treatment, suggesting that pMVs may either exert a preventive or early-stage effect, potentially by modulating cellular pathways or environments before exposure to LPS, and directly counteract the LPS injury. Similarly, the MVs derived from *L. reuteri* DSM 17938 were found to be able to dampen the inflammatory response induced by *Staphylococcus aureus* in peripheral blood mononuclear cells⁵⁶. Among the identified metabolites, lactate is recognized as an immune modulator, influencing the function of immune cells within the tissue microenvironment, both in normal and pathological conditions. For instance, it reduced the release of proinflammatory cytokines by LPS-stimulated RAW 264.7 macrophages; however, it also induced the expression of inflammatory genes in human monocyte-derived macrophages⁶⁴. Moreover, both succinate and citrate play a pivotal role in modulating inflammation and influencing immunity⁶⁵. Particularly, in LPS-stimulated macrophages as well as in cancer models, succinate accumulation activates a cascade that leads to exacerbation of inflammation and enhanced tumor survival and growth; moreover, a citrate increase has been also found, suggesting its involvement in the activation of inflammatory response. Choi et al. also showed that citrate was able to counteract the pro-inflammatory effects induced by LPS, through a modulation of oxidative stress and inflammatory factors⁶⁶. These findings suggest that the effects of *L. reuteri* DSM 17938 MVs in RAW 264.7 macrophages may be due to the contribution of diverse metabolites, among which organic acids; however, the possible involvement of other unidentified compounds, which may also explain the different potency of pMVs and bMVs in the pre-treatment, cannot be excluded.

Altogether this evidence suggests an interest in *L. reuteri* DSM 17938 MVs as immunoregulatory and anti-inflammatory factors; nevertheless, additional and more targeted evaluations are needed to gain a deeper understanding of the mechanisms underpinning these effects, to assess their in vivo impact, and to explore their potential implications for human health.

NMR-based metabolomic analysis

To date, the metabolite characterization of *L. reuteri* vesicles has not been reported, as most of the attention has been focused on the corresponding protein content¹⁸. In this paper, we present the first metabolite mapping and characterization of *L. reuteri* vesicles, using NMR. A similar approach was reported for assessing the metabolites within MVs from *Lactobacillus crispatus* and *Lactobacillus gasseri*⁶⁷.

By applying NMR spectroscopy on freshly prepared *L. reuteri* DSM 17938 vesicle samples, using 2D experiments and literature data^{68,69}, we identified six organic acids (acetate, lactate, malate, citrate, formate and succinate), nine amino acids (alanine, valine, glycine betaine, isoleucine, leucine, glycine, phenylalanine, tyrosine and tryptophan) and choline (Table S1). All the listed metabolites were identified and quantified in bMVs, whereas tyrosine and tryptophan were not detected in pMVs. From a quantitative point of view for each metabolite, bMVs were characterized by a higher concentration with respect to pMVs. Organic acids represented the most abundant class of compounds in vesicle samples, with lactate being the most abundant acid, measured at concentrations of 713 µg/mL and 183 µg/mL in bMVs and pMVs, respectively (Table 1). SCFAs represent a crucial point in the continuous cross-feeding and cross-talking among the diverse inhabitants of the microbiota because of their positive effects on the intestinal barrier function, anti-inflammatory properties, and the contribution of daily energy needs⁷⁰. Moreover, the presence of high amounts of lactate is an expected result and represents a positive factor considering the potential use of these vesicles for pharmaceutical purposes. In fact, the synergistic antibacterial activity of lactic acid in presence of other biologically active metabolites has been largely demonstrated⁷¹ and recently D-lactate produced by *Lactobacillus* was shown to regulate gut homeostasis in mice reducing liver fibrosis⁷². It is noteworthy to underline that, up to now, no studies regarding an NMR-based metabolite comparison among planktonic and biofilm MVs have been carried out. Considering the rich

Metabolite	pMVs	bMVs
Lactate	183.02	713.74
Acetate	12.85	19.07
Succinate	14.73	51.99
Citrate	23.88	80.77
Malate	6.63	23.08
Formate	0.45	0.83
Leucine	5.96	20.61
Isoleucine	2.76	11.41
Valine	4.49	15.85
Alanine	18.78	46.60
Glycinebetaine	1.60	5.79
Glycine	15.02	54.20
Tyrosine	–	1.67
Phenylalanine	1.49	9.41
Tryptophan	–	1.56
Choline	0.08	0.33

Table 1. Quantitative results obtained from NMR analysis of freshly prepared *L. reuteri* DSM 17938 vesicle samples subtracted from their blank (PBS). Results are reported as $\mu\text{g/ml}$ of sample. “–” means “not detected” or “not assigned”.

information here obtained, the application of metabolite profile analysis to compare different vesicle groups can be of great interest to better understand their potential activities and uses.

Regarding amino acids, alanine and glycine were measured as the most abundant metabolites. The presence of this class of compounds in the analyzed vesicles can represent an important starting point regarding the potential application of MVs for pharmaceutical purposes. In particular, putative antiviral effect of *L. crispatus* and *L. gasseri* extracellular vesicles have been reported⁶⁷; the authors statistically correlated the above-mentioned biological activity to the high content of some amino acids, including methionine, hypoxanthine, asparagine, glutamate, and glycine.

Proteomic analysis of MVs

To highlight possible functional properties of *L. reuteri* DSM 17938 pMVs and bMVs, freshly prepared vesicles were separately extracted to recover identical amounts of proteins⁷³, which were subjected to proteomic analysis according to the Tandem Mass Tag (TMT)-based approach⁷⁴. Resulting mass spectrometric data were subjected to database search against a *L. reuteri* repository (UniProtKB) leading to the identification of common 296 proteins in pMVs and bMVs, among which 87 showed a fold change ≥ 1.5 depending on the vesicle type. No specific proteins were identified in pMVs that were not assigned in bMVs, and vice versa. Quantitative proteomic data are reported in **Supplementary Table S2**.

Regarding the nature of all the proteins present in pMVs and bMVs, results generally confirmed previous observations on lysed *L. reuteri* vesicles^{60,75}, with variations possibly depending on the different proteomic technologies used in this and other studies. A PSort3.0-based prediction⁷⁶ of the subcellular localization of the identified proteins showed that 61.5% of them were predicted to be cytoplasmic proteins, 18.6% membrane components, 2.4% secreted proteins, while 17.9% had an unknown localization. The high percentage of cytoplasmic proteins here identified in vesicles was not surprising based on the methodological approach and according to previous studies on other Gram-positive and -negative bacteria^{60,75,77–79}, and may derive from a passive molecular packaging phenomenon during membrane vesicle formation. According to the distribution of biological functions analyzed by GO annotation, most of the identified *L. reuteri* proteins were classified as metabolic and proteolytic enzymes, DNA/RNA-binding proteins, membrane components, chaperone and ribosomal proteins, which are involved in bacterial metabolic, molecular transport, transcription and translation, signaling and stress response pathways (Table 2). In contrast, Pang and colleagues⁵⁶ used a surface shaving-based method and described a significantly greater proportion of proteins of DSM 17938-derived MVs that were predicted to be secreted. We found that several cytosolic proteins identified in *L. reuteri* pMVs and bMVs were previously reported as “moonlighting”^{80–82}, which are highly conserved cytoplasmic proteins that exhibit a different biological function when released or attached to the bacterial cell wall. This is in line with the results of the previously mentioned surface shaving study, in which the authors described several moonlighting proteins to be localized on the surface of the membrane vesicles of *L. reuteri* DSM 17938⁵⁶.

Notably, some of the bacterial proteins identified in pMVs and bMVs were already reported being vesicle mediators of immune/inflammatory responses in the host or associated with beneficial effects of probiotic organisms; they included ABC-type antimicrobial peptide transport system (ATPase component), elongation factor Tu (EF-Tu), chaperonins GroEL and GroES, enolase and mucus adhesion promoting protein (MapA), the latter also being named collagen-binding protein (CnBP)⁵⁶. The ABC-type antimicrobial peptide transport system belongs to the group of transporters potentially involved in bacteriocin/antimicrobial peptide export, self-immunity and resistance, and it was described influencing the local microbial ecology^{75,83}. Moonlighting

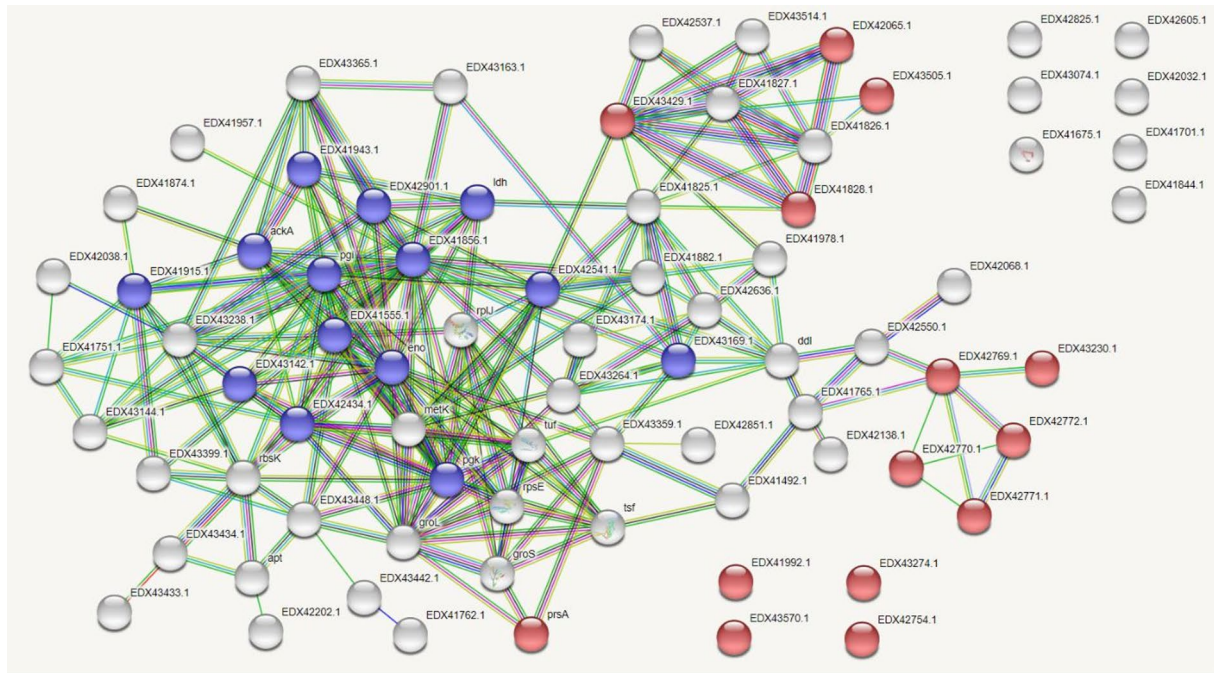
KEGG pathways				
Pathway	Description	Count in network	Strength	FDR
Map00261	Monobactam biosynthesis	4 of 4	0.94	0.0393
Map00020	Citrate cycle (TCA)	5 of 7	0.80	0.0388
Map00010	Glycolysis/Gluconeogenesis	18 of 35	0.65	4.14e-05
Map00030	Pentose phosphate pathway	11 of 22	0.64	0.0030
Map01200	Carbon metabolism	23 of 52	0.59	1.50e-05
Map00190	Oxidative phosphorylation	8 of 18	0.59	0.0305
Map00620	Pyruvate metabolism	17 of 40	0.57	0.00041
Map00270	Cysteine and methionine metabolism	11 of 28	0.54	0.0132
Map00640	Propanoate metabolism	9 of 24	0.52	0.0388
Map01120	Microbial metabolism in diverse environments	40 of 111	0.50	3.36e-07
Map01230	Biosynthesis of amino acids	24 of 68	0.49	0.00014
Map03010	Ribosome	19 of 59	0.45	0.0026
Map01110	Biosynthesis of secondary metabolites	57 of 234	0.33	7.10e-06
Map01100	Metabolic pathways	116 of 617	0.22	3.36e-07

Table 2. Functional analysis of whole proteins identified in freshly prepared *L. reuteri* DSM 17938 pMVs and bMVs. Proteins identified within the UniProtKB *L. reuteri* repository (296 proteins in number) were subjected to functional enrichment based on KEGG database. Top-14 enriched pathways are reported. Shown is the pathway code, the corresponding description, count in network, strength and false discovery rate (FDR).

protein EF-Tu has previously been identified in vesicles of various pathogenic and probiotic bacteria^{77,84–90}. As a cytoplasmic factor, EF-Tu is involved in protein translation; when expressed on the extracellular surface of bacteria, it has shown alternative functions including the stimulation of immune responses and promotion of adhesion and invasion⁸⁷. It was speculated that EF-Tu acts as an immunogenic factor that triggers antibody responses^{88,89} and as a binding effector to macrophages through its interaction with fibronectin⁹⁰. Some studies have also demonstrated that EF-Tu mediates the attachment of lactobacilli to mucins and intestinal cells, participating in the regulation of gut homeostasis by evoking a proinflammatory response in HT-29 cells⁹¹. The same capability of binding to mammalian fibronectin was also reported for another bacterial moonlighting protein, namely enolase⁸⁰. When exposed on the bacterial membrane, moonlighting chaperones GroES and GroEL have been shown to act like adhesins sustaining the microorganism binding to the host tissues, also exerting a stimulation of the immune system^{92,93}. In addition, GroEL was demonstrated to induce tolerogenic dendritic cells and mediate TLR-2 dependent immunoregulatory effects^{94,95}. Finally, MapA/CnBP was shown to participate in the binding of *L. reuteri* to collagen, mucus and Caco-2 cells^{96,97} and it was recently detected on *L. reuteri* DSM 17938 MVs⁵⁶. Taken together, these findings confirmed that pMVs and bMVs carry multiple immunoregulatory proteins, as previously suggested by other researchers^{57,60}, potentially explaining their effect on regulating phagocytosis in LPS-induced RAW 264.7 macrophages (Fig. 7).

Quantitative proteomics recognized 87 proteins that showed a fold change ≥ 1.5 in pMVs and bMVs, consistent with the notion that vesicle content may differ depending on the bacterial phenotype, the mode of growth, and presumably the age of the broth culture⁹⁸. Fifty-nine proteins showed higher levels in pMVs, while twenty-eight had a higher concentration in bMVs. Among the proteins over-represented in pMVs, worth mentioning are some of the above-discussed mediators of immune/inflammatory responses, already associated with beneficial interactions of probiotics, namely EF-Tu and MapA. Additional proteins worth to mention include: (i) four Penicillin-Binding Proteins (PBPs) and peptidoglycan hydrolases, which are involved in cell wall biogenesis⁹⁹ and have been suggested to have a possible role in vesicle formation^{56,100}; (ii) universal stress proteins and thiol peroxidase that are involved in the general response of bacteria to abiotic stresses. In pMVs, augmented levels were also observed for proteins involved in bacterial cell division/elongation, like DivIVA domain protein¹⁰¹, and carbohydrate metabolism, such as lactose and galactose permease, fructose permease, fructokinase, beta-phosphoglucomutase, UDP-glucose 4-epimerase, pyruvate kinase, and two phosphoglycerate kinase isoforms. Various proteases with different substrate specificity were also highly represented in pMVs, namely carboxypeptidase A0 A1 C2GEW9, zinc metalloprotease rseP, peptidase M23 family, dipeptidase PepV and aminopeptidase PepN. Some of the above-mentioned components have already been reported to contribute to the growth of bacteria in their planktonic state^{102,103}.

In the group of proteins more abundant in bMVs, worth mentioning are the above-reported moonlighting proteins associated with the binding to other molecules/cells and/or the mediation of host immune response, namely GroEL, GroES and enolase. GroEL was already demonstrated to play a key role in the lactobacilli colonization of organic surfaces and biofilm development^{104,105}. A similar function was also ascribed to enolase, which was demonstrated highly affecting the ability of *L. plantarum* to produce biofilm¹⁰⁶. In the same functional context, several metabolic enzymes with augmented levels in bMVs are also worth mentioning, namely 6-phosphogluconate dehydrogenase (PGDH), ornithine transcarbamylase, guanosine monophosphate reductase (GMPr), inosine 5'-monophosphate dehydrogenase (IMPDH), L-lactate dehydrogenase (LDH) and aldehyde dehydrogenase (ALDH) (NAD) family protein. PGDH converts 6-phosphogluconate to ribulose 5-phosphate within the pentose phosphate pathway¹⁰⁷, which was recently shown to impact metabolism, energy and



A

KEGG Pathways				
pathway	description	count in network	strength	false discovery rate
map00010	Glycolysis / Gluconeogenesis	8 of 35	0.81	0.0053
map00030	Pentose phosphate pathway	5 of 22	0.81	0.0370
map00640	Propanoate metabolism	5 of 24	0.77	0.0430
map00270	Cysteine and methionine metabolism	5 of 28	0.7	0.0463
map01200	Carbon metabolism	9 of 52	0.69	0.0055
map00620	Pyruvate metabolism	6 of 40	0.63	0.0463
map01230	Biosynthesis of amino acids	9 of 68	0.57	0.0244
map01120	Microbial metabolism in diverse environments	14 of 111	0.55	0.0053
map01110	Biosynthesis of secondary metabolites	17 of 234	0.31	0.0456
map01100	Metabolic pathways	34 of 617	0.19	0.0430

(less ...)

Annotated Keywords (UniProt)				
keyword	description	count in network	strength	false discovery rate
KW-0732	Signal	14 of 81	0.69	0.00034

B

nucleotide output in *S. aureus*, strongly affecting biofilm formation and resistance to stress stimuli¹⁰⁸. Similarly, ornithine transcarbamylase has recently been demonstrated to participate in the degradation of arginine in *Staphylococcus epidermidis*¹⁰⁹ by catalyzing the formation of ornithine and carbamoyl phosphate¹¹⁰; arginine has a key role in the regulation of cell growth and biofilm formation, as shown in *Streptococcus gordonii*¹¹¹. GMPR and IMPDH are involved in the synthesis of adenine-guanine nucleotides and have been described to greatly affect bacterial proliferation^{112,113}. LDH usually catalyzes the conversion of pyruvic acid to lactic acid¹¹⁴, but it has also been shown to promote the production of phenyl lactic acid, having antimicrobial activity against fungi and bacteria¹¹⁵. Finally, ALDH has already been described to be involved in stress responses in both pathogenic and non-pathogenic bacteria^{116,117}. Based on these proteomic observations and the measured levels of extracellular DNA (eDNA) present on the surface of *L. reuteri* DSM 17938 bMVs²², which has already been demonstrated to be involved in cell aggregation and biofilm formation in *Helicobacter pylori*^{118,119}, we hypothesize that the above-reported vesicular proteins, eDNA and ultimately the bMVs may act as synergistic effectors of microbial adhesion and aggregation, promoting biofilm development and sustaining the corresponding phenotype.

STRING analysis of differentially represented proteins in *L. reuteri* pMVs and bMVs allowed the prediction of a functional protein association map, which was characterized by a ramified network including 77 knots and linking together 66 components, plus 11 non-associated species (Fig. 8A). The involvement of the most differentially represented proteins in this network emphasized the occurrence of a functional assembly bridging different components from specific deregulated metabolic pathways/molecular processes possibly associated with physiological differences of the bacterium having its planktonic or biofilm phenotype. Functional analysis of the components reported in Fig. 8A (according to the KEGG metabolic pathway classification) highlighted selective enrichment of proteins involved in glycolysis, metabolism of sulfur-containing amino acids, pyruvate metabolism, biosynthesis of amino acids and microbial metabolism in different environments (Fig. 8B). Functional analysis of the same proteins, according to annotated keywords in UniProtKB database, highlighted a selective enrichment of bacterial components involved in signaling.

◀ **Fig. 8.** STRING analysis of differentially represented proteins present in *L. reuteri* DSM 17938 pMV and bMV. Panel (A). Protein interaction network of differentially represented proteins (87 in number) identified in freshly prepared *L. reuteri* pMV and bMV. Functional protein associations were based on the corresponding data recorded in the STRING database. Medium-confidence interactions (0.4) are shown. Proteins involved in microbial metabolism in diverse environments and bacterial signaling are shown in blue and red, respectively. ackA, acetate kinase; EDX43163.1, aldo/keto reductase; EDX43448.1, malate dehydrogenase; EDX41751.1, ROK family protein; EDX42770.1, hypothetical protein LOC688242; prsA, ppic-type peptidyl-prolyl cis-trans isomerase; EDX43142.1, 6-phosphogluconate dehydrogenase, decarboxylating; EDX41882.1, putative aspartate aminotransferase; eno, phosphopyruvate hydratase; EDX41874.1, Udp-glucose 4-epimerase; EDX41675.1, histone-like DNA-binding protein wrapping DNA to stabilize it; EDX43505.1, substrate-binding region of ABC-type glycine betaine transport system; EDX42754.1, mannosyl-glycoprotein endo- β -N-acetylglucosamidase; rplJ, ribosomal protein L10; EDX41915.1, phosphoglucomutase/phosphomannomutase alpha/beta/alpha domain I; EDX43238.1, alcohol dehydrogenase GroES domain protein; EDX41957.1, acyltransferase 3; EDX43169.1, cysteine synthase/cystathionine beta-synthase family protein; EDX42851.1, mannosyl-glycoprotein endo-beta-N-acetylglucosamidase; EDX41492.1, membrane-associated zinc metalloproteinase M50; EDX41826.1, polar amino acid ABC transporter, inner membrane subunit; EDX43399.1, beta-phosphoglucomutase; EDX41844.1, putative transcriptional regulator, GntR family; EDX42772.1, peptidase M23; EDX42605.1, histidine triad (HIT) protein; tsf, translation elongation factor ts; EDX42550.1, penicillin-binding protein transpeptidase; EDX42636.1, dipeptidase M20; groS, chaperonin cpn10; EDX43274.1, protein of unknown function DUF1002; EDX41827.1, ABC-type polar amino acid transport system, ATPase component; EDX43144.1, PTS system, glucose subfamily, IIA subunit; EDX43264.1, peptidase M1 membrane alanine aminopeptidase; metK, methionine adenosyltransferase; EDX43570.1, conserved hypothetical protein; pgi, glucose-6-phosphate isomerase; EDX43174.1, peptidase M13 neprilysin; EDX42202.1, conserved hypothetical protein; EDX42038.1, conserved hypothetical protein; EDX42068.1, conserved hypothetical protein; EDX42901.1, alcohol dehydrogenase GroES domain protein; EDX43434.1, inosine/uridine-preferring nucleoside hydrolase; EDX42541.1, glutamine synthase; apt, adenine phosphoribosyltransferase; rbsK, ribokinase; EDX43429.1, ABC-type amino acid transport system, permease and periplasmic component - ionotropic glutamate receptor; EDX43433.1, sodium-dependent nucleoside transporter; EDX42434.1, ribulose-phosphate 3-epimerase family protein; EDX42771.1, hypothetical protein; EDX41825.1, cystathionine gamma-synthase; tuf, translation elongation factor tu; EDX42032.1, universal stress protein; ddl, D-alanine/D-alanine ligase; EDX42537.1, nlpA lipoprotein family protein; EDX41856.1, iron-containing alcohol dehydrogenase family protein; EDX43442.1, membrane protein of unknown function UCP033111; EDX41992.1, conserved hypothetical secreted protein; EDX41978.1, ornithine carbamoyltransferase; EDX41828.1, bacterial solute-binding protein 3 family protein; EDX43074.1, ferritin dps family protein; EDX41701.1, protein of unknown function DUF322; EDX43359.1, peptidase S1 and S6 chymotrypsin/Hap; EDX43514.1, nlpA lipoprotein family protein; EDX41943.1, phosphate acetyltransferase; rpsE, ribosomal protein S5; groL, chaperonin GroEL; EDX43230.1, peptidoglycan-binding LysM; EDX42138.1, cell division initiation protein; EDX43365.1, 1,3-propanediol dehydrogenase; EDX41765.1, penicillin-binding protein, 1 A family; EDX42825.1, redoxin domain protein; pgk, phosphoglycerate kinase family protein; EDX41762.1, conserved hypothetical protein; EDX42769.1, hypothetical protein; EDX41555.1, pyruvate kinase family protein; EDX42065.1, glutamine ABC transporter substrate binding component; ldh, L-lactate dehydrogenase. Panel (B). Functional analysis of differently represented proteins identified in freshly prepared *L. reuteri* pMV and bMV. Differentially represented proteins (87 in number) were subjected to functional enrichment based on KEGG pathway database. The top-10 pathways are reported. Shown is the pathway code, the corresponding description, count in network, strength and false discovery rate (FDR).

Preliminary vesicle stability studies using reflectance colorimetry

Organoleptic properties of a mixture or a dispersed system are often subjected to rapid physicochemical changes, which are related to different deep modification or degradation processes. Color analysis was recently applied to different systems with the aim to study the corresponding changes over time in relation to product quality and stability¹⁶. In this context, different review studies have explained how CIEL*a*b* color space can be used to monitor microbiological and physicochemical parameters, so that color results can directly be used as prediction parameters to evaluate the shelf-life of a product^{120–122}. Above-mentioned color changes were often associated with microbial proteolytic and lipolytic activities, as well as with independent Maillard reaction and/or oxidation processes.

On this basis, a rapid and inexpensive technique, such as colorimetric analysis, was here used to evaluate the shelf-life of *L. reuteri* DSM 17938 MVs samples. To this purpose, freshly prepared pMV and bMV were monitored for their color properties after 0, 2 and 4 weeks of storage at 4 °C (Fig. 9A and B, respectively); corresponding blank samples were also analyzed as control (Fig. 9C). All the recorded color parameters are reported in **Supplementary Table S3**. The data showed color differences among samples, both in terms of elapsed time and of different analyzed samples. pMV remained quite similar and faintly greyish color after 2 weeks (pMV at $t^{2\text{weeks}}$), either with respect to their initial condition (pMV at t^0) and the initial status of the medium (PBS at t^0); in the latter case, the calculated color difference ΔE value was 1.82. Conversely, they showed an evident browning after 4 weeks (pMV at $t^{4\text{weeks}}$), with a darker and more yellow color, and a ΔE value of 16.41. This color difference can be considered even more significant, as the medium after 4 weeks (PBS at $t^{4\text{weeks}}$) showed an opposite trend of bleaching, already visible after 2 weeks (PBS at $t^{2\text{weeks}}$). Conversely, bMV both after 2 and 4 weeks (bMV at $t^{2\text{weeks}}$ and $t^{4\text{weeks}}$) showed a very little color difference either with respect to their initial

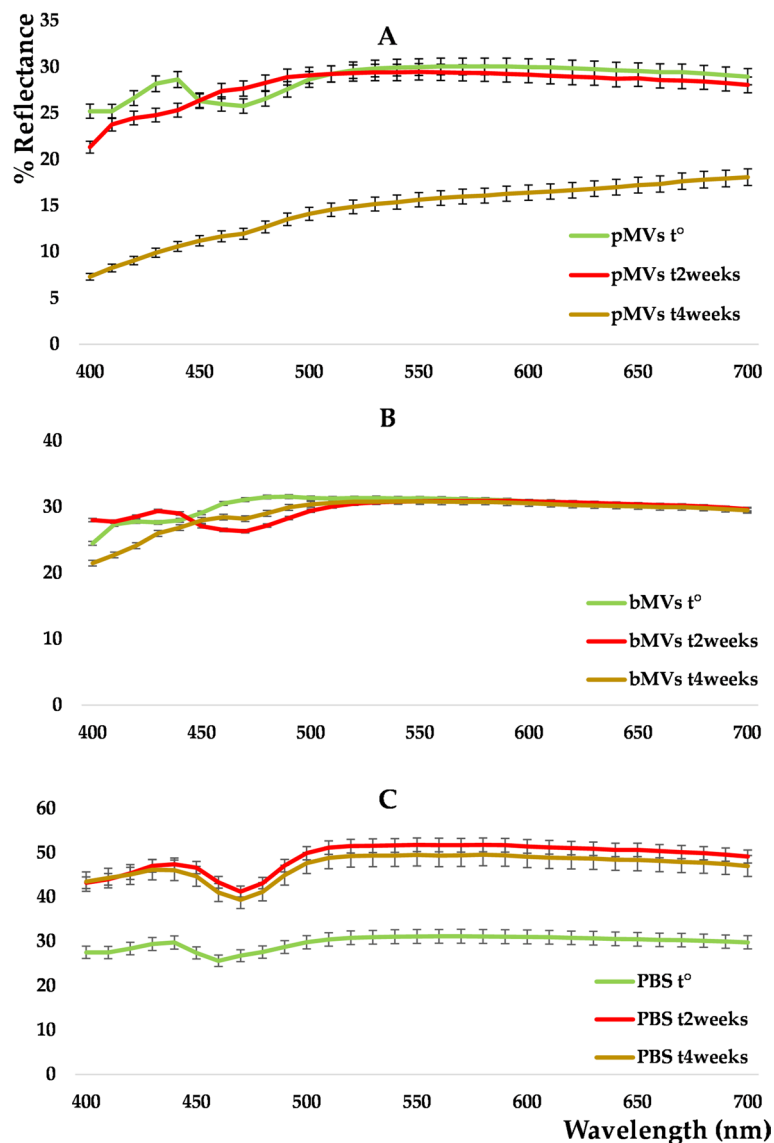


Fig. 9. Reflectance curves of *L. reuteri* DSM 17938 related to membrane vesicles of the planktonic phenotype (pMVs; Panel A), membrane vesicles of biofilm phenotype (bMVs; Panel B) and control samples (PBS; Panel C) after 0 (t^0 , green), 2 (t^{2weeks} , red) and 4 (t^{4weeks} , ocher) weeks of storage at 4 °C. The measurements were carried out at least in triplicate, and the results are reported as mean values standard deviation.

condition (bMVs at t^0) ($\Delta E = 2.24$ and 2.13 , respectively), and to the medium after 0 weeks (PBS at t^0), with $\Delta E = 0.33$ and 1.45 , respectively, thus denoting better stability over time. This trend was confirmed by the reflectance spectra where a general overlapping of the curves was observed only for bMVs (Fig. 9B). To our knowledge, no studies have been reported in the literature, where CIEL*a*b* parameters were used to assess stability of membrane vesicles. In addition, colorimetric analysis can also be utilized to monitor turbidity, as it assesses both light absorption and reflectance in a sample. This property is closely related to the turbidity of the suspension and can provide indirect insights into changes in the concentration or stability of suspended components, such as membrane vesicles. While the absence of significant ΔE variations suggests potential stability of MVs over time, we recognize that colorimetric analysis alone cannot fully confirm vesicle integrity. Without positive control or additional size/concentration data, these results should be considered preliminary and a limitation of this study. However, the use of CIEL*a*b* parameters has been previously validated in literature for shelf-life evaluation in various biological and pharmaceutical systems, supporting its value as a rapid screening tool. Recent studies support the application of colorimeters and spectrophotometers in assessing turbidity alongside color to evaluate physical stability in solutions with dispersed particles^{123,124}. The observed variations in ΔE between pMVs and bMVs align with the distinct metabolomic and proteomic profiles identified through NMR and proteomic analyses. Specifically, the greater color stability of bMVs may reflect their higher concentrations of metabolites and structurally significant proteins, contributing to increased resistance to degradation or aggregation over

time. Conversely, pMV, characterized by lower metabolite content and differing protein compositions, may be more susceptible to physicochemical changes, influencing the recorded color variations.

Conclusions

This study describes the biochemical characterization and a preliminary functional analysis of pMV and bMV isolated from *L. reuteri* DSM 17938. Considering their possible application in postbiotics formulation, the experiments in the *G. mellonella* model allowed to obtain preliminary results regarding the in vivo toxicity of vesicles. The data obtained in this work demonstrated that *L. reuteri* DSM 17938 pMV and bMV did not show toxicity at the tested concentration, corresponding to 10^8 MVs/larva. As stated above, the maximum dosage is strictly dependent on the initial count of the samples, evaluated via NTA analysis. Authors recognize that this could be a limitation of the experimental design here used and consider the possibility to further investigate the effect of higher doses over *G. mellonella*. However, this first screening is a valuable starting point to deepen the understanding of the in vivo effect of MVs.

Despite the antiproliferative properties described for other lactobacilli postbiotics in colon cancer cells^{3,4}, *L. reuteri* DSM 17938 MVs only weakly affected the viability of pancreatic, biliary, liver and mammary cancer cells, as well as that of noncancerous cholangiocytes, after both short and long-term treatments. This suggests a low in vitro anticancer power of the MVs, at least in the tested cell models; further studies could be carried out to clarify their cytotoxic effect in other experimental models, especially in colorectal cancer cells. Moreover, under our experimental conditions, pMV and bMV were both able to affect phagocytosis in LPS-induced RAW 264.7 macrophages, emphasizing possible immunomodulatory characteristics. Our results confirmed recent observations on *L. reuteri* MVs as extracellular structures able to maintain the intestinal immune homeostasis against LPS-induced inflammatory responses in broilers⁶⁰. NMR-based metabolomic analysis of pMV and bMV demonstrated the occurrence of engulfed organic acids and amino acids, whereas bMV contained the highest concentrations. Proteomic analysis of pMV and bMV provided a molecular snapshot of the corresponding bacterial phenotype, highlighting molecular processes and metabolic pathways variably represented in each microorganism physiological state. At the same time, proteomics highlighted specific components possibly exerting signaling functions toward their cellular targets, and molecules acting as mediators of immune/inflammatory responses in the host. The vesicle-mediated character of the delivery system associated with pMV and bMV ensures that the latter molecules could reach target cells protected from the degradation by exogenous enzymes. Differential analysis of pMV and bMV expanded knowledge deriving from previous studies on MVs from *L. reuteri*^{60,75}, and demonstrated significant quantitative composition differences between protein cargos, whether secreted from the bacterial planktonic or biofilm phenotype. This original information correlates well with other dedicated studies on other Gram-positive bacteria^{102,103,125,126}. At the same time, authors recognize that, due to the protocol used for the MVs isolation, further analysis should be taken into account regarding the vesicles isolated from the biofilm phenotype: the presence of the EPS biofilm matrix can promote the formation of vesicles aggregates which can be retained during the filtration process leading to underestimated results, thus, the authors reserve the right to carry out additional investigations to improve the isolation method and disrupt possible aggregates.

The above reported results indicate that *L. reuteri* pMV and bMV have a promising potential as postbiotics modulating the immune/inflammatory responses in the host. Accordingly, novel dedicated studies are encouraged to ascertain the functional properties of *L. reuteri* pMV and bMV, with the aim to definitively support their use in nutraceutical and food industries.

Materials and methods

Bacterial strains and culture conditions

L. reuteri DSM 17938 was kindly provided by BioGaia AB (Stockholm, Sweden) and used in the study. The bacteria were plated on DeMan, Rogosa, and Sharpe agar (MRSA; Oxoid Limited, Hampshire, UK), and incubated at 37 °C, for 24 h, in an anaerobic atmosphere (Anaerogen Pak Jar, Oxoid Ltd.).

MVs isolation and *L. reuteri* DSM 17,938 MVs characterization and quantification

L. reuteri DSM 17938 pMV and bMV, were isolated from the planktonic and biofilm bacterial phenotypes as previously described²². Briefly, *L. reuteri* DSM 17938 was incubated anaerobically overnight in MRSB under shaking conditions. After incubation, the broth culture was diluted in fresh medium to obtain an optical density (OD_{600}) of 0.10 corresponding to 10^7 CFU/ml, transferred into 90 mm diameter TC-treated Petri dishes (Nunc™ Cell Culture/Petri Dishes, Thermo Fisher Scientific) and incubated at 37 °C anaerobically for 24 h, without shaking. After incubation, the supernatant of each petri dish, containing non-adherent cells, was collected, while the biofilm was washed with PBS, then scraped and harvested in fresh PBS. Planktonic and biofilm suspensions thus obtained were centrifuged for 20 min at $4,000 \times g$ at 4 °C and subsequently filtered with 0.22 µm cellulose membrane filters (Corning, New York, NY, USA) to ensure getting a Cell-Free Supernatant (CFS). To isolate vesicles, both planktonic and biofilm CFS were centrifuged at 50,000 rpm for 2 h at 4 °C using a Beckman Coulter Optima XL-100 K ultracentrifuge (Beckman Coulter, USA), washed with PBS and ultra-centrifuged for the second time at the same conditions. Planktonic and biofilm MVs pellets (pMV and bMV) were resuspended in fresh PBS and characterized and quantified by using Nanoparticle Tracking Analysis (NTA). After isolation, they were resuspended in PBS and directly tracked with the NanoSight NS300 system (NanoSight™ technology, Malvern, UK). The analysis was performed at the ALFATEST laboratory (Milan, Italy), according to the company's standard operating procedure (Dilution factor – 1:200; laser – 488 nm; camera level – 16; syringe pump speed – 80; detection threshold – 4). To observe both pMV and bMV, the vesicles suspension was distributed on a formvar-carbon-coated grid (Electron Microscopy Sciences, Hatfield, United Kingdom), and

negatively stained with phosphotungstic acid solution (1% v/v). Samples were then analyzed with a Talos L120 C-G2 TEM (Thermo Fisher Scientific).

Evaluation of the toxicity of *L. reuteri* DSM 17938 membrane vesicles over *G. mellonella*

MVs were tested over the *G. mellonella* wax moth model to evaluate the corresponding *in vivo* toxicity. *G. mellonella* larvae were kindly provided by Prof. Maria Luisa Dindo (Department of Agricultural and Food Science, University of Bologna) and stored in dark, at 20 °C²³. Larvae weighing within the range of 200–250 mg were used for the experiment. Each larva was injected in the third left proleg using a Hamilton syringe (Hamilton, Nevada, USA) and received a total volume of 10 µL of pMVs and bMVs. Both pMVs and bMVs were resuspended in phosphate buffer saline (PBS). Each group consisted of 10 larvae, and the groups included: (i) pMVs-treated larvae; (ii) bMVs-treated larvae; (iii) larvae injected with PBS; (iv) untreated larvae (not injected). Considering the initial MVs count, larvae received the highest achievable dose of vesicles corresponding to 10⁸ MVs/head. Another group, consisting of larvae injected with 100% DMSO, was included in order to validate the injection procedure and to mimic the outcome of a toxic effect (positive control) due to the fact that kills the larvae few minutes after the injection. As an additional positive control, larvae were infected with *Staphylococcus aureus* ATCC 43300 (10⁶, 10⁵ and 10⁴ CFU/larva), a pathogen that allows to observe the reduction of survival through time. Lastly, larvae were also challenged with *L. reuteri* DSM 17938 (10⁶, 10⁵ and 10⁴ CFU/larva) to compare probiotic with pathogen. After the injection, larvae were housed in petri dishes, at 37 °C, and were monitored daily for 4 days to score mortality. Two independent experiments were performed.

Cell cultures

Mz-ChA-1, HepG2 and H69 cells were kindly provided by Prof. G. Alpini (Indiana University School of Medicine, Indianapolis, IN) and Prof. R. Mancinelli (Dept. of Anatomical, Histological, Forensic and Orthopedic Sciences, Sapienza University of Rome). Bx-PC3, HepG2, MDA-MB-468 and RAW 264.7 cells were purchased from Interlab Cell Line Collection (IRCCS San Martino Policlinico Hospital, Genova, Italy). The cells were cultured under standard conditions (37 °C and 5% CO₂ atmosphere), in the recommended media¹⁵, which were renewed twice a week. To evaluate cytotoxicity and phagocytic abilities, the cells were allowed to grow into a 96-well microplate (2 × 10⁴ cells/well) for 24 h after seeding, and then subjected to the treatment with progressive dilutions of pMVs and bMVs for further 24 h and 72 h.

After treatments, the 3-(4,5-dimethylthiazol-2-yl)-2,5-diphenyl tetrazolium bromide (MTT) assay was performed to determine the cytotoxic effects of the treatments. Briefly, 10 µl of 5 mg/mL MTT solution was added to each well, and the plate was incubated at 37 °C for 80 min. Thereafter, the culture medium was discarded, and 200 µl of DMSO was added to each well to dissolve the formazan crystals, directly correlated with cell viability, whose absorbance was measured at 595 nm using a microplate reader (Epoch Microplate Spectrophotometer, BioTek).

Phagocytic abilities of RAW 264.7 macrophages were evaluated in terms of capacity to incorporate and accumulate neutral red (NR) dye within the cells. To this end, NR dye (50 µg/mL) was added to cells for 30 min; then, cells were washed twice in PBS to remove any residual dye and incubated at 4 °C with a 1:1 mixture of ethanol and glacial acetic acid (200 µL/well) for further 120 min to enable the release of NR dye taken up by lysosomes. Thereafter, the neutral red absorbance was measured at 515 nm by an Epoch microplate spectrophotometer (BioTek). The ability of MVs to modulate neutral red uptake by RAW 264.7 cells was assessed under both basal conditions and following the LPS stimulation. To this end, two different protocols were applied: a pre-treatment of 24 h with MVs followed by a 24 h of LPS stimulation, and a co-treatment in which MVs and LPS were administered simultaneously.

To ensure reliable results, the experiments were performed in triplicate for each experiment, with at least two independent experiments conducted. The reduction in cell viability induced by the treatment was evaluated by comparison with the number of viable cells in the vehicle control (1X PBS). A treatment was considered cytotoxic when the cell viability was less than 70% with respect to the control²⁵. Data are expressed as mean ± SE (*n* = 6). A concentration–response curve was obtained using Hill equation, according to previous methods¹²⁷. A significant lowering (*p* < 0.05) in cell viability by treatments with respect to the vehicle control was evaluated by one-way analysis of variance (one-way ANOVA), followed by Dunnett's multiple comparison post-test. Statistical analysis was performed by GraphPad Prism™ (Version 5.00) software (GraphPad Software, Inc., San Diego, CA, USA).

NMR-based metabolomic analysis

One mL of each sample was lyophilized and dissolved in 750 µL of 200 mM phosphate buffer/D₂O, containing 1.4 mM 3-(trimethylsilyl)propionic acid sodium salt (TSP) as internal standard. To lyse vesicles, each solution was sonicated at room temperature for 15 min and centrifuged for 15 min (6000 × *g*, at 20 °C); finally, 700 µL of each solution were transferred into a 5 mm NMR tube. Analyses were carried out on a Jeol JNM-ECZ 600R equipped with a Jeol 5 mm FG/RO DIGITAL AUTOTUNE probe. Mono-dimensional ¹H and bi-dimensional ¹H-¹H TOCSY, ¹H-¹³C HSQC and ¹H-¹³C HMBC NMR experiments were carried out using the previously reported conditions.

Proteomic analysis

Pellets from pMVs and bMVs were solved with the appropriate amount of lysis buffer (8 M urea, 1% w/v SDS, containing protease inhibitor cocktail). Lysis was performed by sonication on ice for 2 min, and then the samples were kept on ice for additional 30 min. Supernatants were recovered by centrifugation at 6000 × *g* for 15 min, at 4 °C. For quantitative proteomics, protein concentration of samples was determined using the BCA Protein assay kit (Thermo Fisher Scientific), according to manufacturer's instructions.

An aliquot of each protein sample (100 µg) was adjusted to a 100 µL final volume with 100 mM TEAB, and then reduced with 5 µL of 200 mM tris (2-carboxyethylphosphine), for 60 min, at 55 °C. Protein samples were then alkylated by adding 5 µL of 375 mM iodoacetamide for 30 min, at 25 °C, in the dark. Alkylated proteins were then precipitated by addition of 6 vol. of cold acetone, pelleted by centrifugation at 8000 × g, for 10 min, at 4 °C, and air-dried. Each sample was digested with freshly prepared trypsin (ratio of enzyme to protein 1:50) in 100 mM TEAB, at 37 °C, overnight. Resulting peptides from each protein sample were labelled with the TMT Label Reagent Set (Thermo-Fisher Scientific, USA) according to the matching pMVs-TMT6-126, bMVs-TMT6-127, at 25 °C, according to manufacturer's instructions. After 1 h of reaction, 8 µL of 5% w/v hydroxylamine was added in each tube and mixed for 15 min to quench the derivatization reaction. For a set of comparative experiments, tagged peptide mixtures were mixed in equal molar ratios (1:1) and vacuum-dried under rotation. Then, pooled TMT-labelled peptide mixtures were suspended in 0.1% trifluoroacetic acid and fractionated by using the Pierce™ High pH Reversed-Phase Peptide fractionation kit (Thermo-Fisher Scientific) to remove unbound TMT reagents and reduce sample complexity, according to manufacturer's instructions. After fractionation, eight fractions of TMT-labelled peptides were collected, vacuum-dried and finally reconstituted in 0.1% formic acid for subsequent mass spectrometric analysis.

TMT-labelled peptide fractions were analyzed on a nanoLC-ESI-Q-Orbitrap-MS/MS platform consisting of an UltiMate 3000 HPLC RSLC nano system (Dionex, USA) coupled to a Q-ExactivePlus mass spectrometer through a Nanoflex ion source (Thermo Fisher Scientific). Peptides were loaded on an Acclaim PepMap TM RSLC C18 column (150 mm × 75 µm ID, 2 µm particles, 100 Å pore size) (Thermo-Fisher Scientific), and eluted with a gradient of solvent B (19.92/80/0.08 v/v/v water/acetonitrile/formic acid) in solvent A (99.9/0.1 v/v water/formic acid), at a flowrate of 300 nL/min. The gradient of solvent B started at 5%, increased to 60% over 125 min, raised to 95% over 1 min, remained at 95% for 8 min, and finally returned to 5% in 1 min, with a column equilibrating step of 20 min before the subsequent chromatographic run. The mass spectrometer operated in data-dependent mode, using a full scan (m/z range 375–1500, nominal resolution of 70,000), followed by MS/MS scans of the 10 most abundant ions. MS/MS spectra were acquired in a scan m/z range 110–2000, using a normalized collision energy of 32%, an automatic gain control target of 100,000, a maximum ion target of 120 ms, and a resolution of 17,500. A dynamic exclusion value of 30 s was also used. Quadruplicate analysis of each sample was performed.

All MS and MS/MS raw data files per sample were merged for protein identification and relative protein quantification into ProteomeDiscoverer vs. 2.4 software (Thermo Scientific), enabling the database search by Mascot algorithm v. 2.4.2 (Matrix Science, UK) using the following criteria: *L. reuteri* UniProtKB protein database (72,034 protein sequences, 06/2022) including the most common protein contaminants; carbamidomethylation of Cys and TMT6plex modification of lysine and peptide N-terminus as fixed modifications; oxidation at Met, deamidation at Asn and Gln, pyroglutamate formation at Gln as variable modifications. Peptide mass tolerance was set to ±10 ppm and fragment mass tolerance to ±0.02 Da. Proteolytic enzyme and maximum number of missed cleavages were set to trypsin and 2, respectively. Protein candidates were considered confidently identified when they were assigned based on at least two sequenced peptides having an individual Mascot Score ≥25. For quantification, ratios of TMT reporter ion intensities in the MS/MS spectra from raw datasets were used to calculate fold changes between samples. Results were filtered to 1% false discovery rate (FDR). Proteomic data were deposited to the ProteomeXchange Consortium via the PRIDE partner repository with the dataset identifier PXD035326.

Protein cell localization, functional and interaction analysis was performed with PSort3.0 software, Kyoto Encyclopedia of Genes and Genomes (KEGG) database^{128,129} and STRING database¹³⁰ resources, respectively.

Colorimetric analysis

pMVs and bMVs samples in PBS at the standard concentration of 1.83×10^{11} particles/mL and 7.87×10^{10} particles/mL respectively, were analyzed, such as, for their color character with a X-Rite MetaVue™ colorimeter as previously described¹³¹. Measurements were performed under the same experimental conditions on freshly prepared vesicle samples (t^0), and then after 2 weeks ($t^{2\text{weeks}}$) and 4 weeks ($t^{4\text{weeks}}$) after their storage at 4 °C. After 4 weeks, pMVs samples presented traces of mold and the experiment was stopped. Control samples contained only PBS. Cylindrical coordinates C^*_{ab} , h_{ab} and the color distances (ΔE) were calculated with respect to the corresponding data of the control samples at the initial time (t^0), as previously reported¹³². The analysis was performed on two independent samples, each measured in triplicate.

Data availability

Data is provided within the text and supplementary information files.

Received: 22 July 2024; Accepted: 22 May 2025

Published online: 29 May 2025

References

1. Ranjha, M. M. A. N. et al. Nutritional and health potential of probiotics: A review. *Appl. Sci.* **11**, 11204 (2021).
2. Hill, C. et al. The international scientific association for probiotics and prebiotics consensus statement on the scope and appropriate use of the term probiotic. *Nat. Rev. Gastroenterol. Hepatol.* **11**, 506–514 (2014).
3. Thorakkattu, P. et al. Postbiotics: current trends in food and pharmaceutical industry. *Foods* **11**, 3094 (2022).
4. Hernández-Granados, M. J. & Franco-Robles, E. Postbiotics in human health: possible new functional ingredients?. *Food Res. Int.* **137**, 109660 (2020).
5. Alaei, M., Aghakhani, F., Falsafi, S., Mazaheri, H. & Behrouzi, A. Introduce a novel Post-Biotic against *Pseudomonas aeruginosa* biofilm formation using *Escherichia coli* Nissle1917 outer membrane vesicles. *BMC Res. Notes.* **16**, 201 (2023).

6. Molina-Tijeras, J. A., Gálvez, J. & Rodríguez-Cabezas, M. E. The Immunomodulatory properties of extracellular vesicles derived from probiotics: A novel approach for the management of Gastrointestinal diseases. *Nutrients* **11**, 1038 (2019).
7. Salminen, S. et al. The international scientific association of probiotics and prebiotics (ISAPP) consensus statement on the definition and scope of postbiotics. *Nat. Rev. Gastroenterol. Hepatol.* **18**, 649–667 (2021).
8. Ji, J. et al. Probiotics, Prebiotics, and Postbiotics in Health and Disease. *MedComm* (2023).
9. Shi, Y. et al. Extracellular vesicles from *Lactocaseibacillus paracasei* PC-H1 inhibit HIF-1 α -Mediated Glycolysis of Colon cancer. *Future Microbiol.* **19**, 227–239 (2024).
10. El Far, M. S. et al. Promising biotherapeutic prospects of different probiotics and their derived postbiotic metabolites: In-Vitro and histopathological investigation. *BMC Microbiol.* **23**, 122 (2023).
11. Savino, F. et al. Regulatory T cells and Toll-Like receptor 2 and 4 mRNA expression in infants with colic treated with *Lactobacillus reuteri* DSM17938. *Benef Microbes.* **9**, 917–926 (2018).
12. Savino, F. et al. *Lactobacillus reuteri* DSM 17938 Probiotics May Increase CC-Chemokine Receptor 7 Expression in Infants Treated With for Colic. *Front Pediatr* **7**, (2019).
13. Ojetti, V. et al. The effect of *Lactobacillus reuteri* supplementation in adults with chronic functional constipation: a randomized, Double-Blind, Placebo-Controlled trial*. *J. Gastrointest. Liver Dis.* **23**, 387–391 (2014).
14. Gutierrez-Castrellon, P. et al. Diarrhea in preschool children and *Lactobacillus reuteri*: A randomized controlled trial. *Pediatrics* **133**, e904–e909 (2014).
15. Maccelli, A. et al. Correlation between the antimicrobial activity and metabolic profiles of cell free supernatants and membrane vesicles produced by *Lactobacillus reuteri* DSM 17938. *Microorganisms* **8**, 1653 (2020).
16. Vitale, I. et al. Antibiofilm Activity and NMR-Based Metabolomic Characterization of Cell-Free Supernatant of *Limosilactobacillus reuteri* DSM 17938. *Front Microbiol* **14**, (2023).
17. Xiao, M., Li, G. & Yang, H. Microbe-Host Interactions: Structure and Functions of Gram-Negative Bacterial Membrane Vesicles. *Front Microbiol* **14**, (2023).
18. Krzyżek, P., Marinacci, B., Vitale, I. & Grande, R. Extracellular vesicles of probiotics: shedding light on the biological activity and future applications. *Pharmaceutics* **15**, 522 (2023).
19. González-Lozano, E. et al. Novel horizons in postbiotics: Lactobacillaceae extracellular vesicles and their applications in health and disease. *Nutrients* **14**, 5296 (2022).
20. Domínguez Rubio, A. P., D'Antoni, C. L., Piuri, M. & Pérez, O. E. Probiotics, Their Extracellular Vesicles and Infectious Diseases. *Front Microbiol* **13**, (2022).
21. Repetto, G., del Peso, A. & Zurita, J. L. Neutral red uptake assay for the Estimation of cell viability/cytotoxicity. *Nat. Protoc.* **3**, 1125–1131 (2008).
22. Grande, R. et al. Detection and physicochemical characterization of membrane vesicles (MVs) of *Lactobacillus reuteri* DSM 17938. *Front. Microbiol.* **8**, 1040 (2017).
23. Gallorini, M. et al. Immunophenotyping of hemocytes from infected *Galleria Mellonella* larvae as an innovative tool for immune profiling, infection studies and drug screening. *Sci. Rep.* **14**, 759 (2024).
24. Hanušová, V., Boušová, I. & Skálová, L. Possibilities to increase the effectiveness of doxorubicin in Cancer cells killing. *Drug Metab. Rev.* **43**, 540–557 (2011).
25. International Organization for Standardization/ANSI. (ISO Standard No. 10993–5:2009) Biological Evaluation of Medical Devices Part 5: Tests for in vitro Cytotoxicity. Second edition, Geneva, Switzerland. (2009).
26. Lan, A., Lagadic-Gossman, D., Lemaire, C., Brenner, C. & Jan, G. Acidic extracellular pH shifts colorectal Cancer cell death from apoptosis to necrosis upon exposure to propionate and acetate, major End-Products of the human probiotic propionibacteria. *Apoptosis* **12**, 573–591 (2007).
27. Thoda, C. & Touraki, M. Probiotic-Derived bioactive compounds in colorectal Cancer treatment. *Microorganisms* **11**, 1898 (2023).
28. Bell, H. N. et al. Reuterin in the healthy gut Microbiome suppresses colorectal Cancer growth through altering redox balance. *Cancer Cell.* **40**, 185–200e6 (2022).
29. Gao, C. et al. Gut Microbe-Mediated suppression of Inflammation-Associated Colon carcinogenesis by luminal Histamine production. *Am. J. Pathol.* **187**, 2323–2336 (2017).
30. Cousin, F. J. et al. The probiotic *Propionibacterium freudenreichii* as a new adjuvant for TRAIL-Based therapy in colorectal Cancer. *Oncotarget* **7**, 7161–7178 (2016).
31. Ghanavati, R. et al. Inhibitory effects of lactobacilli cocktail on HT-29 Colon carcinoma cells growth and modulation of the Notch and Wnt/ β -Catenin signaling pathways. *Microb. Pathog.* **139**, 103829 (2020).
32. Salek, F., Mirzaei, H., Khandaghi, J., Javadi, A. & Nami, Y. Apoptosis induction in Cancer cell lines and Anti-Inflammatory and Anti-Pathogenic properties of proteinaceous metabolites secreted from potential probiotic *Enterococcus faecalis* KUMS-T48. *Sci. Rep.* **13**, 7813 (2023).
33. Ma, E. L. et al. The anticancer effect of probiotic *Bacillus polyfermenticus* on human Colon cancer cells is mediated through ErbB2 and ErbB3 Inhibition. *Int. J. Cancer.* **127**, 780–790 (2010).
34. Xu, F. et al. The Efficacy of Prevention for Colon Cancer Based on the Microbiota Therapy and the Antitumor Mechanisms With Intervention of Dietary *Lactobacillus*. *Microbiol Spectr* **11**, (2023).
35. Chen, Z. et al. Microbiota in Cancer: Molecular Mechanisms and Therapeutic Interventions. *MedComm* (2023).
36. Iyer, C. et al. Probiotic *Lactobacillus reuteri* promotes TNF-Induced apoptosis in human myeloid Leukemia-Derived cells by modulation of NF- κ B and MAPK signalling. *Cell. Microbiol.* **10**, 1442–1452 (2008).
37. Kahouli, I. et al. Characterization of *L. reuteri* NCIMB 701359 Probiotic Features for Potential Use as a Colorectal Cancer Biotherapeutic by Identifying Fatty Acid Profile and Anti-Proliferative Action Against Colorectal Cancer Cells. *Drug Des. Open. Access* **5**, (2016).
38. Suri, K., D'Souza, A., Huang, D., Bhavsar, A. & Amiji, M. Bacterial extracellular vesicle applications in Cancer immunotherapy. *Bioact Mater.* **22**, 551–566 (2023).
39. Liang, A., Korani, L., Yeung, C. L. S., Tey, S. K. & Yam, J. W. P. The Emerging Role of Bacterial Extracellular Vesicles in Human Cancers. *J Extracell. Vesicles* **13**, (2024).
40. Gurunathan, S., Ajmani, A. & Kim, J. H. Extracellular nanovesicles produced by *Bacillus licheniformis*: A potential anticancer agent for breast and lung Cancer. *Microb. Pathog.* **185**, 106396 (2023).
41. Keyhani, G., Hosseini, H. M. & Salimi, A. Effect of extracellular vesicles of *Lactobacillus rhamnosus* GG on the expression of CEA gene and protein released by colorectal Cancer cells. *Iran. J. Microbiol.* **14**, 90–96 (2022).
42. Behzadi, E., Mahmoodzadeh Hosseini, H. & Imani Fooladi, A. A. The inhibitory impacts of *Lactobacillus rhamnosus* GG-Derived extracellular vesicles on the growth of hepatic Cancer cells. *Microb. Pathog.* **110**, 1–6 (2017).
43. Shi, Y., Meng, L., Zhang, C., Zhang, F. & Fang, Y. Extracellular vesicles of *Lactocaseibacillus paracasei* PC-H1 induce colorectal Cancer cells apoptosis via PDK1/AKT/Bcl-2 signaling pathway. *Microbiol. Res.* **255**, 126921 (2021).
44. An, J. & Ha, E. M. Extracellular vesicles derived from *Lactobacillus plantarum* restore chemosensitivity through the PDK2-Mediated glucose metabolic pathway in 5-FU-Resistant colorectal Cancer cells. *J. Microbiol.* **60**, 735–745 (2022).
45. Zhang, J. et al. Antitumorigenic potential of *Lactobacillus*-derived extracellular vesicles: p53 succinylation and glycolytic reprogramming in intestinal epithelial cells via SIRT5 modulation. *Cell. Biol. Toxicol.* **40**, 66 (2024).

46. Abedi, A., Tafvizi, F., Jafari, P. & Akbari, N. The Inhibition effects of *Lentilactobacillus buchneri*-derived membrane vesicles on AGS and HT-29 Cancer cells by inducing cell apoptosis. *Sci. Rep.* **14**, 3100 (2024).
47. Yi, S. et al. Harnessing *Lactobacillus reuteri* -Derived extracellular vesicles for multifaceted Cancer treatment. *Small* <https://doi.org/10.1002/smll.202406094> (2024).
48. Wang, T. et al. Lactate-induced Protein Lactylation: A Bridge Between Epigenetics and Metabolic Reprogramming in Cancer. *Cell Prolif* **56**, (2023).
49. Icard, P., Simula, L., Zahn, G., Alifano, M. & Mycielska, M. E. The dual role of citrate in Cancer. *Biochim. Biophys. Acta - Rev. Cancer.* **1878**, 188987 (2023).
50. Kuo, C. C., Wu, J. Y. & Wu, K. K. Cancer-derived extracellular succinate: a driver of Cancer metastasis. *J. Biomed. Sci.* **29**, 93 (2022).
51. Gu, J. et al. Tumor metabolite lactate promotes tumorigenesis by modulating MOESIN lactylation and enhancing TGF- β signaling in regulatory T cells. *Cell. Rep.* **40**, 111122 (2022).
52. Liu, W. et al. Lactate regulates cell cycle by remodelling the anaphase promoting complex. *Nature* **616**, 790–797 (2023).
53. Casas-Benito, A., Martínez-Herrero, S. & Martínez, A. Succinate-Directed approaches for Warburg Effect-Targeted Cancer management, an alternative to current treatments?? *Cancers (Basel)*. **15**, 2862 (2023).
54. Kasarci, G., Ertugrul, B., Iplik, E. S. & Cakmakoglu, B. The apoptotic efficacy of succinic acid on renal Cancer cell lines. *Med. Oncol.* **38**, 144 (2021).
55. Ates, G., Vanhaecke, T., Rogiers, V. & Rodrigues, R. M. Assaying Cellular Viability Using the Neutral Red Uptake Assay. *Cell Viability Assays: Methods and Protocols* 19–26. https://doi.org/10.1007/978-1-4939-6960-9_2 (2017).
56. Pang, Y. et al. Extracellular Membrane Vesicles From *Limosilactobacillus reuteri* Strengthen the Intestinal Epithelial Integrity, Modulate Cytokine Responses and Antagonize Activation of TRPV1. *Front Microbiol* **13**, (2022).
57. Mata Forsberg, M. et al. Extracellular membrane vesicles from lactobacilli dampen IFN- γ responses in a Monocyte-Dependent manner. *Sci. Rep.* **2019**. **9**, 1–13 (2019).
58. Kim, W. et al. *Lactobacillus plantarum*-Derived extracellular vesicles induce Anti-Inflammatory M2 macrophage polarization in vitro. *J. Extracell. Vesicles.* **9**, 1793514 (2020).
59. Hao, H. et al. Effect of extracellular vesicles derived from *Lactobacillus plantarum* Q7 on gut microbiota and ulcerative colitis in mice. *Front. Immunol.* **12**, 5167 (2021).
60. Hu, R. et al. *Lactobacillus reuteri*-Derived Extracellular Vesicles Maintain Intestinal Immune Homeostasis Against Lipopolysaccharide-Induced Inflammatory Responses in Broilers. *Journal of animal science and biotechnology* **12**, 25 (2021).
61. Walter, J., Britton, R. A. & Roos, S. Host-Microbial Symbiosis in the Vertebrate Gastrointestinal Tract and the *Lactobacillus reuteri* Paradigm. *Proc. Natl. Acad. Sci. U. S. A* (2011).
62. Mu, Q., Tavella, V. J. & Luo, X. M. Role of *Lactobacillus reuteri* in human health and diseases. *Front. Microbiol.* **9**, 315828 (2018).
63. Yao, Y., Xu, X. H. & Jin, L. Macrophage Polarization in Physiological and Pathological Pregnancy. *Front Immunol* **10**, (2019).
64. Yang, K. et al. Lactate Suppresses Macrophage Pro-Inflammatory Response to LPS Stimulation by Inhibition of YAP and NF- κ B Activation via GPR81-Mediated Signaling. *Front Immunol* **11**, (2020).
65. Mills, E. & O'Neill, L. A. J. Succinate: a metabolic signal in inflammation. *Trends Cell. Biol.* **24**, 313–320 (2014).
66. Choi, E. Y., Kim, H. J. & Han, J. S. Anti-inflammatory effects of calcium citrate in RAW 264.7 cells via suppression of NF- κ B activation. *Environ. Toxicol. Pharmacol.* **39**, 27–34 (2015).
67. Ñahui Palomino, R. A. et al. Extracellular vesicles from symbiotic vaginal lactobacilli inhibit HIV-1 infection of human tissues. *Nat. Commun.* **10**, 1–14 (2019).
68. Spano, M. et al. Metabolomic Profiling of Fresh Goji (*Lycium barbarum* L.) Berries from Two Cultivars Grown in Central Italy: A Multi-Methodological Approach. *Molecules* **26**, 5412 (2021).
69. Spano, M. et al. A multimethodological approach for the chemical characterization of edible insects: the case study of *Acheta domesticus*. *Foods* **12**, 2331 (2023).
70. Daisley, B. A. et al. Emerging connections Between gut Microbiome bioenergetics and chronic metabolic diseases. *Cell. Rep.* **37**, 110087 (2021).
71. Sanam, M., Detha, A. & Rohi, N. Detection of antibacterial activity of lactic acid bacteria, isolated from Sumba Mare's milk, against *Bacillus cereus*, *Staphylococcus aureus*, and *Escherichia coli*. *J. Adv. Vet. Anim. Res.* **9**, 53 (2022).
72. Santos, A. A. et al. Host miRNA-21 promotes liver dysfunction by targeting small intestinal *Lactobacillus* in mice. *Gut Microbes.* **12**, 1840766 (2020).
73. Xu, H. et al. Adhesion characteristics and dual transcriptomic and proteomic analysis of *Lactobacillus reuteri* SH23 upon Gastrointestinal fluid stress. *J. Proteome Res.* **20**, 2447–2457 (2021).
74. Lombardi, N. et al. *Trichoderma* Applications on Strawberry Plants Modulate the Physiological Processes Positively Affecting Fruit Production and Quality. *Front Microbiol* **11**, 1364 (2020).
75. Dean, S. N., Leary, D. H., Sullivan, C. J., Oh, E. & Walper, S. A. Isolation and characterization of *Lactobacillus*-Derived membrane vesicles. *Sci. Rep.* **9**, 877 (2019).
76. Yu, N. Y. et al. PSORTb 3.0: improved protein subcellular localization prediction with refined localization subcategories and predictive capabilities for all prokaryotes. *Bioinformatics* **26**, 1608–1615 (2010).
77. Lee, E. Y. et al. Gram-Positive Bacteria produce membrane vesicles: Proteomics-Based characterization of *Staphylococcus aureus*-Derived membrane vesicles. *Proteomics* **9**, 5425–5436 (2009).
78. Mashburn-Warren, L. M. & Whiteley, M. Special delivery: vesicle trafficking in prokaryotes. *Mol. Microbiol.* **61**, 839–846 (2006).
79. Faddetta, T. et al. *Streptomyces coelicolor* Vesicles: Many Molecules To Be Delivered. *Appl Environ. Microbiol* **88**, (2022).
80. Castaldo, C. et al. Surface displaced Alfa-Enolase of *Lactobacillus plantarum* is a fibronectin binding protein. *Microb. Cell. Fact.* **8**, 1–10 (2009).
81. Henderson, B. & Martin, A. Bacterial virulence in the moonlight: multitasking bacterial moonlighting proteins are virulence determinants in infectious disease. *Infect. Immun.* **79**, 3476–3491 (2011).
82. Jeffery, C. J., Protein, & Moonlighting. What is it, and Why is it Important?. *Philos Trans. R Soc. B* **373** (1738), 20160523 (2018).
83. Gebhard, S. A. B. C. Transporters of antimicrobial peptides in Firmicutes Bacteria – Phylogeny, function and regulation. *Mol. Microbiol.* **86**, 1295–1317 (2012).
84. Prados-Rosales, R. et al. Mycobacteria release active membrane vesicles that modulate immune responses in a TLR2-Dependent manner in mice. *J. Clin. Invest.* **121**, 1471–1483 (2011).
85. Wang, X., Thompson, C. D., Weidenmaier, C. & Lee, J. C. Release of *Staphylococcus aureus* extracellular vesicles and their application as a vaccine platform. *Nat. Commun.* **9**, 1–13 (2018).
86. Olaya-Abril, A. et al. Characterization of protective extracellular Membrane-Derived vesicles produced by *Streptococcus pneumoniae*. *J. Proteom.* **106**, 46–60 (2014).
87. Harvey, K. L., Jarocki, V. M., Charles, I. G. & Djordjevic, S. P. The diverse functional roles of elongation factor Tu (Ef-tu) in microbial pathogenesis. *Front. Microbiol.* **10**, 2351 (2019).
88. Torres, A. N. et al. Deciphering additional roles for the EF-Tu, l-Asparaginase II and ompt proteins of Shiga Toxin-Producing *Escherichia coli*. *Microorganisms* **8**, 1–16 (2020).
89. Nieves, W. et al. Immunospesific responses to bacterial elongation factor Tu during *Burkholderia* infection and immunization. *PLoS One.* **5**, 1–12 (2010).

90. Dallo, S. F. et al. Association of *Acinetobacter baumannii* EF-Tu With Cell Surface, Outer Membrane Vesicles, and Fibronectin. *ScientificWorldJournal* **2012**, 128705 (2012).
91. Granato, D. et al. Cell Surface-Associated Elongation Factor Tu Mediates the Attachment of *Lactobacillus johnsonii* NCC533 (Lal) to Human Intestinal Cells and Mucins. *Infection and immunity* **72**, 2160–2169 (2004).
92. Pessione, E. Lactic acid Bacteria contribution to gut microbiota complexity: lights and shadows. *Front. Cell. Infect. Microbiol.* **2**, 86 (2012).
93. Jeffery, C. J. Intracellular/Surface moonlighting proteins that aid in the attachment of gut microbiota to the host. *AIMS Microbiol.* **5**, 77–86 (2019).
94. Wang, X. et al. CD4⁺ CD25⁺ Treg induction by an HSP60-Derived peptide SJMHE1 from *Schistosoma Japonicum* is TLR2 dependent. *Eur. J. Immunol.* **39**, 3052–3065 (2009).
95. Al-Nedawi, K. et al. Gut commensal microvesicles reproduce parent bacterial signals to host immune and enteric nervous systems. *FASEB J.* **29**, 684–695 (2015).
96. Miyoshi, Y., Okada, S., Uchimura, T. & Satoh, E. A. Mucus adhesion promoting protein, MapA, mediates the adhesion of *Lactobacillus reuteri* to Caco-2 human intestinal epithelial cells. *Biosci. Biotechnol. Biochem.* **70**, 1622–1628 (2006).
97. Roos, S. et al. A collagen binding protein from *Lactobacillus reuteri* is part of an ABC transporter system?? *FEMS Microbiol. Lett.* **144**, 33–38 (1996).
98. Schooling, S. R. & Beveridge, T. J. Membrane vesicles: an overlooked component of the matrices of biofilm. *J. Bacteriol.* **188**, 5945–5957 (2006).
99. Zapun, A., Contreras-Martel, C. & Vernet, T. Penicillin-Binding proteins and β -Lactam resistance. *FEMS Microbiol. Rev.* **32**, 361–385 (2008).
100. Uddin, M. J. et al. The role of bacterial membrane vesicles in the dissemination of antibiotic resistance and as promising carriers for therapeutic agent delivery. *Microorganisms* **8**, 670 (2020).
101. Martinez-Goikoetxea, M. & Lupas, A. N. A conserved motif suggests a common origin for a group of proteins involved in the cell division of Gram-Positive Bacteria. *PLoS One.* **18**, e0273136 (2023).
102. Allan, R. N. et al. Pronounced metabolic changes in adaptation to biofilm growth by *Streptococcus pneumoniae*. *PLoS One.* **9**, e107015 (2014).
103. Dumitrache, A. et al. Specialized activities and expression differences for *Clostridium thermocellum* biofilm and planktonic cells. *Sci. Rep.* **7**, 43583 (2017).
104. De Angelis, M., Siragusa, S., Campanella, D., Di Cagno, R. & Gobbetti, M. Comparative proteomic analysis of biofilm and planktonic cells of *Lactobacillus plantarum* DB200. *Proteomics* **15**, 2244–2257 (2015).
105. De Angelis, M., Calasso, M., Cavallo, N., Di Cagno, R. & Gobbetti, M. Functional proteomics within the genus *Lactobacillus*. *Proteomics* **16**, 946–962 (2016).
106. Vastano, V. et al. The *Lactobacillus plantarum* Eno A1 enolase is involved in immunostimulation of Caco-2 cells and in biofilm development. *Adv. Exp. Med. Biol.* **897**, 33–44 (2016).
107. Sundaramoorthy, R. et al. Crystal structures of a bacterial 6-Phosphogluconate dehydrogenase reveal aspects of specificity, mechanism and mode of Inhibition by analogues of High-Energy reaction intermediates. *FEBS J.* **274**, 275–286 (2007).
108. Kim, J., Kim, G. L., Norambuena, J., Boyd, J. M. & Parker, D. Impact of the Pentose phosphate pathway on metabolism and pathogenesis of *Staphylococcus aureus*. *PLOS Pathog.* **19**, e1011531 (2023).
109. Gómez-Chávez, F. et al. The extracellular vesicles from the commensal *Staphylococcus epidermidis* ATCC12228 strain regulate skin inflammation in the Imiquimod-Induced psoriasis murine model. *Int. J. Mol. Sci.* **22**, 13029 (2021).
110. Fang, R. et al. Improving the enzyme property of ornithine transcarbamylase from *Lactobacillus Brevis* through Site-Directed mutation. *LWT* **133**, 109953 (2020).
111. Jakubovics, N. S. et al. Critical roles of arginine in growth and biofilm development by *Streptococcus gordonii*. *Mol. Microbiol.* **97**, 281–300 (2015).
112. Martinelli, L. K. B. et al. Recombinant *Escherichia coli* GMP reductase: kinetic, catalytic and chemical mechanisms, and thermodynamics of Enzyme–Ligand binary complex formation. *Mol. Biosyst.* **7**, 1289–1305 (2011).
113. Juvale, K., Shaik, A. & Kirubakaran, S. Inhibitors of inosine 5'-Monophosphate dehydrogenase as emerging new generation antimicrobial agents. *Medchemcomm* **10**, 1290–1301 (2019).
114. Rico, J., Yebra, M. J., Pérez-Martínez, G., Deutscher, J. & Monedero, V. Analysis of Ldh genes in *Lactobacillus casei* BL23: role on lactic acid production. *J. Ind. Microbiol. Biotechnol.* **35**, 579–586 (2008).
115. Li, X., Jiang, B., Pan, B., Mu, W. & Zhang, T. Purification and partial characterization of *Lactobacillus species* SK007 lactate dehydrogenase (LDH) catalyzing phenylpyruvic acid (PPA) conversion into phenyllactic acid (PLA). *J. Agric. Food Chem.* **56**, 2392–2399 (2008).
116. Konkitt, M., Choi, W. J. & Kim, W. Aldehyde dehydrogenase activity in *Lactococcus chungangensis*: application in cream cheese to reduce aldehyde in alcohol metabolism. *J. Dairy. Sci.* **99**, 1755–1761 (2016).
117. Singh, S. et al. Aldehyde dehydrogenases in cellular responses to oxidative/electrophilic stress. *Free Radic Biol. Med.* **56**, 89–101 (2013).
118. Grande, R. et al. *Helicobacter pylori* ATCC 43629/NCTC 11639 outer membrane vesicles (OMVs) from biofilm and planktonic phase associated with extracellular DNA (eDNA). *Front. Microbiol.* **6**, 1369 (2015).
119. Grande, R. et al. Selective Inhibition of *Helicobacter pylori* carbonic anhydrases by carvacrol and thymol could impair biofilm production and the release of outer membrane vesicles. *Int. J. Mol. Sci.* **22**, 11583 (2021).
120. Rauh, V. & Xiao, Y. The shelf life of Heat-Treated dairy products. *Int. Dairy. J.* **125**, 105235 (2022).
121. Sicari, V. et al. Shelf-Life evaluation of San Marzano dried tomato slices preserved in extra Virgin Olive oil. *Foods* **10**, 1706 (2021).
122. Putnik, P. et al. Prediction and modeling of microbial growth in minimally processed Fresh-Cut apples packaged in a modified atmosphere: A review. *Food Control.* **80**, 411–419 (2017).
123. Brodgesell, A. & Lipták, B. *8.60 Turbidity, Sludge, and Suspended Solids* 1680 (Process Measurement and Analysis, 2003).
124. Mutanen, J. et al. Measurement of color, refractive index, and turbidity of red wines. *Am. J. Enol. Vitic.* **58**, 387–392 (2007).
125. Vilain, S. & Brözel, V. S. Multivariate approach to comparing Whole-Cell proteomes of *Bacillus cereus* indicates a Biofilm-Specific proteome. *J. Proteome Res.* **5**, 1924–1930 (2006).
126. Planchon, S. et al. Comparative subproteome analyses of planktonic and sessile *Staphylococcus xylosum* C2a: new insight in cell physiology of a Coagulase-Negative *Staphylococcus* in biofilm. *J. Proteome Res.* **8**, 1797–1809 (2009).
127. Di Sotto, A. et al. Modulation of STAT3 signaling, cell redox defenses and cell cycle checkpoints by β -Caryophyllene in cholangiocarcinoma cells: possible mechanisms accounting for doxorubicin chemosensitization and chemoprevention. *Cells* **9**, 858 (2020).
128. Kanehisa, M. K. E. G. G. Kyoto encyclopedia of genes and genomes. *Nucleic Acids Res.* **28**, 27–30 (2000).
129. Kanehisa, M., Sato, Y., Kawashima, M., Furumichi, M. & Tanabe, M. KEGG as a reference resource for gene and protein annotation. *Nucleic Acids Res.* **44**, D457–D462 (2016).
130. Szklarczyk, D. et al. The STRING database in 2023: Protein–Protein association networks and functional enrichment analyses for any sequenced genome of interest. *Nucleic Acids Res.* **51**, D638–D646 (2023).
131. Lasalvia, A. et al. Characterization and Valorization of ‘Sulmona Red Garlic’ Peels and Small Bulbs. Antioxidants (2022).
132. Cairone, F., Carradori, S., Locatelli, M., Casadei, M. A. & Cesa, S. Reflectance colorimetry: A mirror for food Quality—A Mini review. *Eur. Food Res. Technol.* **246**, 259–272 (2020).

Acknowledgements

The Authors gratefully acknowledge BioGaia AB (Stockholm, Sweden) for the donation of the strain used in the present study as well as for supporting the research project. This publication was produced while attending the PhD programme in Innovative Technologies in Clinical Medicine & Dentistry at the University of Chieti-Pescara, Cycle XXXVIII, with the support of a scholarship co-financed by the Ministerial Decree no. 352 of 09.04.2022, based on the NRRP - funded by the European Union - NextGenerationEU - Mission 4 “Education and Research”, Component 2 “From Research to Business”, Investment 3.3, and by the company BioGaia AB Sweden.

Author contributions

R.G. and S.C. designed the project, R.G., S.C., A.D.S., A.S. designed the experiments, discussed the results and drafted the paper. B.M., C.D.A., I.V., V.P., M.G., M.S., M.M., S.F. and F.C. performed the experiment consisting in the isolation of MVs, evaluation of the corresponding toxic and cytotoxic activity, proteomic analysis, analysis of metabolic/color profiles and cell toxicity. R.G., S.C., G.G., S.R., L.E.L. and A.S. drafted the final editing of paper and critically revised the paper.

Funding

This work was supported by the Company BioGaia AB, Stockholm Sweden, and the Ministero Italiano dell’Università e della Ricerca (MIUR) FAR2020 Grant, held by R.G. This research was also funded by the Italian National Research Council for the project “Nutrizione, Alimentazione ed Invecchiamento Attivo (NUTRAGE)” (FOE 2021–2022), and the Agritech National Research Center within the European Union NextGenerationEU program (the National Recovery and Resilience Plan, mission 4, component 2, investment 1.4 – D.D. 1032 del 17/06/2022, project CN00000022). This manuscript reflects only the authors’ views and opinions, neither the European Union nor European Commission can be considered responsible for them.

Declarations

Competing interests

Authors L.E.L., S.R. and G.G. are currently employed by the company BioGaia AB. Authors R.G. and S.C. have received a research grant from Company BioGaia that supported the project. The remaining authors declare no competing interests.

Additional information

Supplementary Information The online version contains supplementary material available at <https://doi.org/10.1038/s41598-025-03823-w>.

Correspondence and requests for materials should be addressed to R.G.

Reprints and permissions information is available at www.nature.com/reprints.

Publisher’s note Springer Nature remains neutral with regard to jurisdictional claims in published maps and institutional affiliations.

Open Access This article is licensed under a Creative Commons Attribution-NonCommercial-NoDerivatives 4.0 International License, which permits any non-commercial use, sharing, distribution and reproduction in any medium or format, as long as you give appropriate credit to the original author(s) and the source, provide a link to the Creative Commons licence, and indicate if you modified the licensed material. You do not have permission under this licence to share adapted material derived from this article or parts of it. The images or other third party material in this article are included in the article’s Creative Commons licence, unless indicated otherwise in a credit line to the material. If material is not included in the article’s Creative Commons licence and your intended use is not permitted by statutory regulation or exceeds the permitted use, you will need to obtain permission directly from the copyright holder. To view a copy of this licence, visit <http://creativecommons.org/licenses/by-nc-nd/4.0/>.

© The Author(s) 2025